ANALYSIS OF MACULAR VOLUME AND THICKNESS IN PRIMARY OPEN ANGLE GLAUCOMA SUSPECTS AND PATIENTS WITH PRIMARY OPEN ANGLE GLAUCOMA USING OPTICAL COHERENCE TOMOGRAPHY

DISSERTATION SUBMITTED FOR M.S (FINAL)

OPHTHALMOLOGY,

THE TAMILNADU Dr. M.G.R MEDICAL UNIVERSITY , CHENNAI,

MARCH2007.

CERTIFICATE

Certified that this dissertation entitled **"ANALYSIS OF MACULAR VOLUME AND THICKNESS IN PRIMARY OPEN ANGLE GLAUCOMA SUSPECTS AND PATIENTS WITH PRIMARY OPEN ANGLE GLAUCOMA USING OPTICAL COHERENCE TOMOGRAPHY''** submitted for M.S (FINAL) Ophthalmology, The Tamilnadu Dr. M.G.R Medical University, Chennai , March 2007, is the bonafide work done by **Dr. Manoj .V** under the direct supervision and guidance in the **Department of Glaucoma Services of Aravind Eye Hospital and post graduate institute of ophthalmology , Madurai** during his residency period from may 2004 to march 2007 .

Dr. S. R. KRISHNA DAS

Chief Glaucoma Services
Aravind eye hospital,
Madurai .

Dr. M. SRINIVASAN

Director and Chief Cornea services ,
Aravind eye hospital ,
Madurai .

ACKNOWLEDGEMENT

I acknowledge with gratitude, the many people who have contributed to the completion of this dissertation.

I sincerely thank my guide **Dr. Krishnadas ,** Chief , Glaucoma Services, Aravind Eye Hospital , Madurai, whose support , patience and care towards me has guided me to the undertaking of this study to a successful completion .

I am very grateful to **Dr .Venkatesh Prajna,** Chief , Department of medical education, for all his help, guidance and support that he has extended me throughout my residency programme.

I express my heartfelt thanks to late **Dr. G .Venkatasamy,** Founder and Former Chairman ,**Dr. P. Namperumalsamy,** the Chairman , **Dr. M .Srinivasan,** the Director and **Dr .G.Natchiar,** Director , HRD whose untiring dedication to the prevention of needless blindness in this community has, and will continue to inspire innumerable young ophthalmologists like me .

I am indebted to **Dr. Sharmila,** Consultant, Glaucoma services and **Dr. Rakhi Mehta**, Fellow in glaucoma, who reviewed my work and provided critical evaluation and support in analyzing this study.

I thank my Biostatistician, **Ms. Mahalakshmi,** for her great effort in analyzing and compiling of the results of this study .I also thank **Mr. Saravanan,** the OCT

technician who helped me in taking the OCT in all the patients included in the study .

This study could not have been completed without the team support of the Glaucoma paramedical staff-the clinic nurses.

I would fail in my duty if I did not thank the patients involved in the study.
I also thank Medianett for their kind cooperation in bringing out this dissertation in a nice and timely manner.

Last but not least I thank my parents, my brother and my friends who were of constant support throughout my life for what I am this day.

CONTENTS

PART – I

PART – II

INTRODUCTION

Glaucoma is one of the leading cause of irreversible blindness in the developing countries and a major health problem in developed countries[1].

The early diagnosis of glaucoma and early detection of its progression are twin challenges the present generation ophthalmologists face[4].

WHO statistics indicate that glaucoma accounts for blindness in 5.1 million people ie 13.5% of global blindness[2].

Since glaucomatous damage is irreversible, prevention of this injury before it occurs is the essential strategy available to those treating the disease.

Primary open angle glaucoma is characterized by chronic progressive optic neuropathy developing in the presence of open angles with characteristic visual field defects and raised intra ocular pressure[3].

In glaucoma the essential pathologic process is the loss of retinal ganglion cells and their axons. Studies have shown that glaucomatous damage to the retinal nerve fiber layer precede functional loss by as much as 5 years[5].

The size and anatomical distribution of retinal ganglion cells varies throughout the posterior pole. Approximately 50% of retinal ganglion cells are located in the macular region 4-5mm from the center of the fovea, with the peak density occurring 750-1100micrometre from the foveal center where the cell density may be 4-6 cell bodies thick .Although cell diameter distribution is variable a skewed distribution towards layer cell diameter (14-16micrometers) exists in the normal retina and such cells have been shown to be selectively lost in human and experimental models of glaucoma.

20% loss of retinal ganglion cells throughout the central 30 degrees of the retina was associated with a 5 dB sensitivity loss with automated perimetry ,a 40% loss corresponded to a 10dB loss in sensitivity .

Glaucomatous cupping of optic disc is subject to variation in interpretation and is not sensitive for identifying small changes[6]. Drawings and photography of the optic nerve head depend on the subjective interpretation of the examiner and are subject to variability in interpretation.

Current diagnostic techniques like retinal and optic nerve head analysis instruments and stereo fundus photography lack sensitivity[6-13].

OPTIC NERVE HEAD ANALYZERS which are developed to quantitatively assess glaucomatous cupping measures optic nerve head rim area and provide indices of optic nerve head structure but can’t reliably differentiate between normal and glaucomatous optic nerve

head and are limited in their ability to detect change over time[7-10].

Improved axial resolution with reduced variability in assessing optic nerve topography is achieved with the **CONFOCAL SCANNING LASER OPHTHALMOSCOPE** which produces optical section of the retina and optic nerve head in a coronal plane.

Cross sectional imaging of the fundus with scanning laser ophthalmoscope is limited by ocular aberrations and the pupil aperture to approximately 300 micrometers of axial resolution[14].

OPTICAL COHERENCE TOMOGRAPHY is useful for the measurement of macular thickness which may be technically easier to measure than nerve fiber layer thickness, as the latter requires a operator to center the scan on the optic nerve in nerve fiber layer thickness scans.

OCT is a non invasive, non contact method that allows cross sectional, invivo imaging of the intra retinal layers[15]. Anatomic layers of the retina can be imaged and quantitative assessment of the macular thickness and peri papillary NFL thickness can be obtained based on the different reflectivity properties of different layers[15,16]. Studies have shown decrease in RNFL thickness using OCT in patients with glaucoma compared to normal healthy eyes[17-21].

Structure based methodologies need to ultimately compare with a gold standard, which

is currently, the automated perimetry. But, glaucoma patients could suffer a loss of retinal ganglion cell axons before an automated perimetry visual field defect is evident[22].

Optical coherence tomography (OCT) provides the highest resolution of tissue thickness among the commercially available tissue imaging modalities.

Quigley and co-workers showed that significant axonal loss may precede the development of visual field defects and identifiable cupping[45-47].

Zeimer et al[75] reported a significant correlation between glaucomatous visual field defects and reductions in macular thickness using a **RETINAL TOPOGRAPHER (RETINAL THICKNESS ANALYZER)** based on the principles of slit lamp biomicroscopy. Significant losses in retinal thickness at the posterior pole of up to 34% were reported to occur in patients with early glaucoma, a mean corrected pattern standard deviation (CPSD) approximately 5.5 dB.

The aim of this study is to use OCT to measure total macular volume/thickness and to use this as an inclusive quantitative assessment of glaucoma and management of glaucoma in the clinical practice.

REVIEW OF LITERATURE

A literature search was done on optical coherence tomography (OCT), OCT on macular thickness and glaucoma the most relevant studies with respect to these topics and this dissertation were selected.

Optical coherence tomography to detect and manage retinal disease and glaucoma .

Glenn J. Jaffe ,Joseph Caprioli .AJO , 2004;137:156-169.

The purpose of the study was to review basic principles of OCT , and to describe its use in the diagnosis and management of retinal diseases and glaucoma . OCT is a imaging technique based on Michelson interferometry . It has been used to identify macular holes, to differentiate macular holes from simulating lesions , to identify macular cysts , vitreo macular traction , sub retinal fluid, pigment epithelial detachment, and choroidal neovascularizations . It is also used to measure macular thickness and RNFL thickness. It has its own limitations of being expensive and image quality is dependent on operator technique and can be degraded in the presence of media opacity. The study concluded , OCT to be a useful imaging technique in the diagnosis and management of retinal diseases and glaucoma .

Quantification of NFL thickness in normal and glaucomatous eyes using OCT.

Joel S. Schuman ,Micheal R. Hee et al. Arch Ophthalmol,.1995;113:586-596.

In this study 59 eyes were studied of 33 subjects, the purpose of the study was to

quantitatively assess the NFL thickness in normal and glaucomatous eyes , and correlate with conventional measurements of the optic nerve structure and function .In the study the NFL thickness as measured by OCT demonstrated a high degree of correlation with functional status of the optic nerve , as measured by VF examination .Neither cupping of the optic nerve nor neuro retinal rim area were as strongly associated with VF loss as was NFL thickness . NFL ,especially in the inferior quadrant , was significantly thinner in glaucomatous eyes than in normal eyes . The study concluded that NFL thickness can be measured using OCT and these measurements provide good structural and functional correlation with known parameters .

Reproducibility of nerve fiber thickness, macular thickness , and optic nerve head measurements using Stratus OCT .

Lelia A .Paunescu,James G. Fujimoto et al .IOVS,2004;45:1716-1724.

In the study 10 eyes of 10 normal subjects were imaged 6 times (3 times before and 3 times after dilatation) per day, and the series was repeated on 3 different days. The purpose of the study was to investigate the reproducibility of the 3rd generation of commercial OCT , OCT-3. The NFL thickness , macular thickness map, and optic nerve head (ONH) parameters in normal eyes were studied . The mean macular thickness was 235 ± 9.8 μm, and the mean RNFL thickness was 98 ± 9 μm. The study showed that OCT had a statistically significant effect on the reproducibility of the mean macular thickness, macular volume and optic nerve head parameters. NFL reproducibility showed mixed results. OCT-3 demonstrated reproducible measurements of NFL thickness, macular thickness and optic nerve head parameters.

Optical coherence tomography (OCT) Macular and Peripapillary RNFL measurements and automated VF.

Gadi Wollstein , Lori L. Price et al. AJO,2004;138:218-225.

A retrospective study of 150 eyes of 101 subjects with glaucoma were analyzed. The study was to investigate the structure –function relationship between OCT macular retinal and peripapillary NFL thickness and automated VF findings. Areas under the receiver operator characteristics for macular thickness were higher in areas corresponding to the VF defect location than the non corresponding locations. Areas under the receiver operator characteristics for peripapillary NFL thickness were higher than for the macular retinal thickness. The study concluded that with OCT it was capable of detecting glaucomatous damage and the macular retinal thickness corresponded with peripapillary NFL thickness; however, peripapillary NFL thickness had higher sensitivity and specificity for the detection of VF abnormalities .

Macular thickness changes in glaucomatous optic neuropathy detected using OCT.

David S. Greenfield, Harmohina Bagga et al. Arch Ophthalmol,2003;121:41-46.

In the study 59 eyes of 59 patients (29 normal and 30 glaucomatous) were studied. The objective of this study was to correlate macular thickness and RNFL thickness in normal and glaucomatous eyes using OCT . In the study mean macular thickness was significantly associated with visual field mean defect , pattern standard deviation and mean RNFL thickness. In glaucomatous eyes with VF loss localized to 1 hemifield, mean macular thickness in the quadrant associated with the field defect was significantly less than in the unaffected quadrant. Mean RNFL thickness in the affected quadrant was significantly thinner than in the unaffected quadrant. Hence it concluded that macular thickness changes are well correlated with changes

in visual function and RNFL structure in glaucoma and may be a surrogate indicator of retinal ganglion cell loss .

Quantitative assessment of structural damage in eyes with localized VF abnormalities .

Harmohina Bagga , David S. Greenfield et al .AJO,2004;137:797-805.

In this study 40 eyes of 40 patients (20 normal and 20 glaucomatous) were studied. The aim of the study was to evaluate the pattern of structural damage in the macula and peripapillary RNFL using OCT and scanning laser polarimetry (SLP-VCC) in glaucomatous eyes with localized VF defects . It was found that diffuse RNFL and retinal ganglion cell loss is present in eyes with localized VF abnormalities. Detection of localized changes in macular thickness is limited by measurement overlap among normal and glaucomatous eyes. The mean RNFL thickness using SLP – VCC and OCT in the non glaucomatous segments of glaucomatous eyes were significantly reduced compared with the thickness measurements in the corresponding segments of age matched normal subjects. But no significant difference in the macular thickness measurements were observed between non glaucomatous and normal segments RNFL thickness in the non glaucomatous segments was abnormal in 75% with SLP – VCC and in 90% with OCT.

Optical coherence tomography of the human retina .

Micheal R. Hee , Puliafito et al . Arch Ophthalmol , 1995;113:325-332.

The objective of the study was to demonstrate optical coherence tomography can be used for high resolution , non invasive imaging of the human retina . OCT can discriminate the cross sectional morphologic features of the fovea and the optic disc ,the layered structure of the retina , and RNFL thickness with 10 micrometers depth resolution . Hence OCT is a potentially

useful technique for high depth resolution , cross sectional examination of the posterior pole of the fundus .

OPTICAL COHERENECE TOMOGRAPHY (OCT)

OCT is a non invasive non contact technique that allows high resolution cross sectional in vivo imaging of the anterior and posterior segments of the eye.

Anatomical layers in the retina can be imaged and quantitative assessment of retinal nerve fiber layer and macular thickness can be performed based on the difference in reflective properties of different layers.

OCT is analogous to CT which uses X-rays and to MRI which uses spin resonance or to an USG –B scan which uses sound waves. OCT uses light for scanning. OCT is a computer assisted precision optical instrument that generates cross sectional images/tomograms of the retina with <10 micrometers axial resolution. Several studies have demonstrated the clinical validity and reproducibility of OCT measurement of macular volume/thickness to detect glaucomatous change[73].

OCT VS USG

1) The principle difference between OCT and USG is that USG uses sound energy and OCT uses light energy for imaging. The speed of light is nearly a million times faster than the speed of sound.This difference permits measurement of structures and distances in the < 10 micrometers scale vs the 100 micrometers scale for USG.
2) OCT does not require contact with the tissue examined, unlike with USG.

MECHANISM OF OCT

OCT contains an INTERFEROMETER that resolves retinal structures by measuring the echo delay time of light that is reflected and back scattered from different microstructural features in the retina.

PRINCIPLE:

OCT works on the principle of **MICHELSON'S LOW COHERENCE LASER INTERFEROMETRY**.

OCT projects a broad band width near infra-red light beam (820-843nm) onto the retina from a super luminescent diode. It then compares the echo time delays of light reflected from the retina with the echo time delays of the same light beam reflected from a reference mirror at known distances.

When the OCT INTERFEROMETER combines the reflected light pulse from the retina and reference mirror, a phenomenon known as INTERFERENCE occurs.

A photo detector detects and measures interference.

The light reflected from the retina consists of multiple echoes ,the distances traveled by various echoes is determined by varying the distance to reference mirror. This produces a change of time delays of the reference light for comparison[73].

The OCT interferometer electronically detects, collects, processes and stores the echo delay pattern from the retina. With each scan pass the OCT captures from 128 – 768 longitudinal (axial) range sample ie A-scans. Each A-scan consists of 1024 data points over 2mm of depth. Thus OCT integrates from 131072-786432 data points to construct a cross

sectional image/tomogram of retinal anatomy[76].

INTERPRETATION:

OCT displays the tomograms in real time using a false colour code scale that represents the degree of light back scattering from tissues at different depths in the retina.

COLOUR CODES:

Blue, Black (dark colours) - regions of minimum relative optical reflectivity.

Red, White (bright colours)- regions of high optical reflectivity.

Deeper Choroid and Sclera represented as weak reflections due to signal attenuation.

Retinal pigment epithelium (RPE) and Chorio-Capillaries as high reflective red layer.

Dark layer immediately anterior to Retinal pigment epithelium is the photo receptor layer.

Middle retinal layer exhibits moderate back scattering.

Nerve fiber layer (NFL) is highly reflective and inner most.

Vitreo retinal interface is well defined due to contrast between NFL and non reflective vitreous[73].

INSTRUMENTATION:

OCT system hardware consists of the module computer unit, flat screen, video monitor, keyboard, mouse and colour inkjet printer.

APPLICATIONS:

OCT analyze the Optic Disc, Retina, NFL, Macula with help of 18 scan acquisition protocols and 18 analysis protocols.

SCANS:

2 basic scan patterns –lines and circles. 3 most commonly used scans are,

FAST OPTICAL DISC

FAST RNFL THICKNESS

FAST MACULAR THICKNESS MAP.

FAST MACULAR THICKNESS MAP:

Six 6mm radial line scans through a common central axis is taken. This protocol is designed for examination of macular thickness as an indicator of glaucoma. It is designed for use with the analysis that measures retinal thickness and to obtain maps of retinal thickness in a circular area centered on the macula[73].

EMBRYOLOGY OF MACULA

Development of macula has unique features. Early in gestation it may be differentiated by an increase in ganglion cells. The axons of these cells elongate such that the ganglion cell bodies become located more peripherally. The nearly horizontally positioned axons thus form the nerve fiber of henle.

Only cones develop with in the macula , no rods develop. These cones are morphologically different from those elsewhere in the retina in that they are taller and thinner. Macular development continues for a few months after birth and is dependent on a light stimulus[71].

ANATOMY OF MACULA

The umbo, foveola, fovea, parafovea and perifovea together constitute the macula or the central area. The central area can be differentiated from the extra-areal periphery by the ganglion cell layer. In the macula, the ganglion cell layer is several cells thick, while in the

extra-areal periphery it is only 1 cell thick.

The macular border coincides with the course of the major temporal arcades and has an approximate diameter of 5.5mm

PARAMETERS OF MACULA

The Diameter of fovea-1.5mm.

The Diameter of parafovea-1mm.

The Diameter of perifovea-3mm.

UMBO, CENTRE OF THE MACULA

The fovea represents an excavation in the retinal centre and consists of a margin, a declivity, a bottom. The bottom corresponds to the foveola , the centre of which is called the UMBO . The umbo represents the precise centre of the macula, the area of the retina that results in the highest visual acuity[71].

The predominant photoreceptor of the foveola and umbo is the cone. The foveal cones result from the centripetal migration of the first neuron and the centrifugal lateral displacement of the second and third neurons during foveal maturation which occurs three months before and three months after term . The central cones because of their high concentration and crowding have their nuclei arranged in multiple layers in a circular shape which resembles a cake ‘‘GATEAU NUCLEAIRE’’. Radiating striae found in the foveal internal limiting membrane are related to henle’s fibers[71].

FOVEOLA

The central cones are surrounded by the foveal bottom/foveola which is approximately 350 microns in diameter and 150 microns in thickness. This avascular area consists of densely packed cones that are elongated and connected by the external limiting membrane. Both umbo and foveola represent the most visible part of the outer retina. The apex to apex arrangement of the optic cup is maintained in the foveola by the processes of mullerian glia that face the apices of the pigment epithelium .The high metabolic needs of the central cones are met by direct contact with the pigment epithelium as well as through the processes of glia whose nuclei lie more peripheral in the inner nuclear layer and closer to the perifoveal vascular arcades[71].

FOVEA

The fovea consists of the thin bottom a 22 degree declivity {the clivus} and a thick margin . The declivity of 22 degree denotes the lateral displacement of the second and third neurons in the inner nuclear layer which includes most of the nuclei of its mullerian glia . The avascular foveola is surrounded by the vascular arcades , a circular system of capillaries . These vessels are located at the level of the internal nuclear layer and leave an avascular zone of 250-600 microns between them .

The declivity is associated with an increase in the basement membrane thickness , which reaches a maximum at the foveal margin . Internal limiting membrane thickness and strength of vitreal attachment are inversely proportional that is adhesion are strongest in the foveola .The margin of the fovea {MARGO FOVEAE} is seen biomicroscopically as a ring like reflection

of the internal limiting membrane which measures 1500 microns in diameter and 0.55mm in thickness[71].

PARAFOVEA

The parafovea is a belt measuring 0.5mm in width and surround the foveal margin. At this distance from the centre of retina features a regular architecture of layers which includes 4-6 layers of ganglion cell and 7-11 layers of bipolar cells.

PERIFOVEA

The perifovea surrounds the parafovea as a belt that measures 1.5mm wide. The region is characterized by several layers of ganglion cells and 6 layers of bipolar cells[71].

MACULAR FUNCTION TESTS

These are required for diagnosing as well as for following up of macular diseases and for evaluating the potential macular function in eyes with opaque media like in cataract , dense vitreous haemorrhage.

The retinal function testing can be divided into PSYCHOPHYSICAL and PHYSIOLOGICAL methods.

A Psychophysical test is subjective. A physical stimulus is presented to the patient and the patient indicates verbally or by other subjective means , his detection of the stimulus.

Physiologic methods are objective. A stimulus is presented and a response parameter is measured by electro-physiological or other means.

PSYCHOPHYSICAL TESTS

1. Visual Acuity.
2. Pupillary Reaction.
3. Photostress test.
4. Amslers grid.
5. Two point discrimination test.
6. Entoptic phenomenon.
7. Tests dependent on macular pigment.
8. Maddox rod test.

9. Colour vision.
10. Foveal flicker sensitivity.
11. Grating psychophysics.
12. Dark adaptation.
13. Perimetry.
14. Laser interferometry.
15. Potential acuity meter.
16. Haidinger's brushes.
17. Maxwell's spot.
18. Koch's yellow filter test.

ELECTROPHYSIOLOGICAL TEST'S

1. Electroretinography(ERG).
2. Electrooculograhy(EOG).
3. Visually evoked response(VER)[71].

PRIMARY OPEN ANGLE GLAUCOMA (POAG)

A) PRE-TRABECULAR :

- Membrane overgrowth –fibrovascular membrane in neovascular glaucoma.

- Endothelial layer , often with descemet like membrane in iridocorneal endothelial syndrome, posterior polymorphous dystrophy , penetrating and non penetrating trauma.
- Epithelial downgrowth.
- Fibrous ingrowth.
- Inflammatory membrane like Fuch's heterochromic iridocyclitis, Luetic interstitial keratitis .

B) TRABECULAR :

- Idiopathic like Chronic open angle glaucoma , Juvenile open angle glaucoma .
- Clogging of trabecular meshwork like

a) RBC

- Haemorraghic glaucoma,
- Ghost cell glaucoma,
- Sickled RBC's .

b) MACROPHAGES

- Haemolytic glaucoma,
- Phacolytic glaucoma.

c) NEOPLASTIC CELLS

- Primary ocular tumours,
- Neoplastic tumours,
- Juvenile xanthogranuloma.

d) PIGMENT PARTICLES

- Pigmentary glaucoma,
- Exfoliation syndrome,
- Malignant melanoma.

e) PROTEINS

- Uveitis,
- Lens induced glaucoma.

f) VISCO ELASTIC AGENTS

- Alfa chymotrypsin induced glaucoma.

g) ALTERATION OF TRABECULAR MESHWORK

- Steroid induced glaucoma,
- Alkali burns.

h) TRAUMA

- Angle recession.

i) INTRA OCULAR FOREIGN BODY

- Haemosiderosis,
- Chalcosis.

C) POST TRABECULAR :

-Obstruction of schlemm's canal like

a) Collapse of canal

b) Raised episcleral venous pressure

- Carotico cavernous fistula,
- Cavernous sinus thrombosis,
- Retrobulbar tumours,
- Thyroid ophthalmopathy,
- SVC obstruction,
- Mediastinal tumours,
- Sturge weber syndrome,
- Familial.

OPTIC NERVE HEAD AND NFL IMAGING IN GLAUCOMA

It was Hermann von helmholtz who invented the ophthalmoscope in 1851 until then the human retina and optic nerve was not visualized[23]. Developments in automated and static perimetry have improved the accuracy and reproducibility of documenting VF defects but patients may lose significant nervous tissue prior to development of detectable VF loss[5].

Therefore the appearance of the optic nerve and adjacent NFL are the best signs of glaucoma's presence or its progression.

Subjective assessment of the ONH cupping are not sufficiently sensitive to detect small changes, especially notches and other local abnormalities and are unable to discriminate between glaucomatous and normal optic nerve head. Drawings of the optic nerve head and stereoscopic optic nerve head photography are clinical methods which are subject to variability in interpretation[24].

Fundus photography was introduced with the development of the Nordenson camera in the early 20th century. Stereoptic disc photos have been used to document changes in the optic nerve appearance over time. Nerve fiber bundles have been demonstrated with the use of red free light. In addition fluorescein angiography has been used to show areas of the optic disc. Although photographs provide a fine pictures of the optic nerve head over time, their interpretation is subjective[25]. Technology has been introduced over the past 2 decades to improve the examination of the optic nerve head, the RNFL and the most recent the macular thickness in the assessment of glaucoma.

OPTIC NERVE HEAD ANALYSIS

PAR IS2000/TOPCON IMAGENET

These were developed to quantitate cupping, to measure neuro retinal rim area and to provide other indices of optic nerve head. Like fundus camera, automated systems used standard fundus camera's optics and could digitize simultaneous stereoimages either directly or from 35mm slides[26]. By using algorithms for image registration and cross correlation to calculate depth values at well matched corresponding points, a three dimensional map of the optic nerve head was created.

RODENSTOCK OPTIC NERVE HEAD ANALYZER

It used a method similar to the PAR instrument, the digital input coming directly from a stereoscopic video camera and was obtained while projecting 2 sets of 7 evenly spaced lines on the optic nerve head[28].

HUMPHREY RETINAL ANALYZER

It uses a similar system but input was from a red free stereoscopic video camera[27].

GLAUCOMASCOPE

The glaucomascope is based on the principle of raster stereography. This instrument

assesses the deviation of projected lines on the optic nerve head to reconstruct 3 dimensional anatomy from a monocular image. It projects 25 parallel horizontal lines onto the optic nerve head at an angle of 90 degrees to the optic nerve head surface , using an infra red light source[29-31] . The lines are deflected proportionately to the depth of the surface .The images are recorded on a video monitor and the deflections are translated into depth values from approximately 8750 data points. A reference surface is used and is calculated from extrapolation of the data from 2 vertical lines 350 microns on either side of the optic nerve head.

These optic nerve head analyzers are not reliable enough to differentiate between normal and glaucomatous optic nerve head and are limited in their ability to detect change over time[7,9-12,32-35]. Although these systems are an attempt to automate and thus increase the objectivity of optic nerve evaluation , their accuracy and reproducibility , are still limited by the optics of the systems and they still rely a great deal on human control and interpretation .

SCANNING LASER OPHTHALMOSCOPY

Compared to the optic nerve head analyzers, improved axial resolution and reduced variability in assessing optic nerve topography is achieved with the confocal scanning laser ophthalmoscope, which produces optical sections of the retina and optic nerve head in a

coronal plane. Scanning systems can be divided into 2 different categories based on the way that they detect the signal reflected back from the scanned object-

CONFOCAL AND NON CONFOCAL SYSTEMS

NON CONFOCAL SYSTEMS

A laser beam from a helium neon , argon or infra red laser illuminates the eye . The beam is focused by the cornea onto the retina with a spot size of approximately 10-20 microns. The optical quality of the eye limits the minimum spot diameter . The laser beam is deflected by a rotating polygon for fast horizontal scanning and a galvanometer for slow vertical scanning to probe the fundus point by point and line by line . A partially reflective mirror separates the light back scattered from the retina and the illumination beam light. The detector receives a time resolved image signal which is displayed on a video monitor[36,37].

A scanning imaging system is advantageous as the contrast is high, due to selective illumination. At any given time only the point on the retina that is to be imaged is illuminated by the laser beam.

CONFOCAL SYSTEMS

The newer scanning laser ophthalmoscopes use a double scanning confocal optical system[38] .The illuminating laser light is scanned across the retina along with the detector system .These confocal scanning microscopes are based on the principle of spot illumination and spot detection; with this type of imaging, only 1 spot on the retina is illuminated at a time through a pinhole aperture[39-41]. A second small confocal aperture allows only light originating from the illuminated retinal area to pass through. The contrast is enhanced more than with non

confocal scanning systems. Because the depth of field is dependent on the size of the detector aperture, depth of field can be varied by altering aperture diameter. When depth of field is reduced, layer by layer imaging is possible within the retina.

RODENSTOCK CONFOCAL SCANNING LASER OPHTHALMOSCOPE

It obtains each focal plane image in one-thirtieth of a second as a 525 horizontal line analog video signal with a field of view of 20-40 degrees and has a focal plane half width thickness of 300 microns[36,38]. Resolution with this system is dependent on laser spot size and imaging pinhole diameter, rather than the optics of a fundus camera. The vertical resolution of depth is related to the spacing of the focal plane images. Although the scanning laser ophthalmoscope predominantly has served the purpose of imaging, the laser scanning tomographer provides added features of 3 dimensional measurements of ocular structure with good reproducibility[42].

The Heidelberg Laser Tomographic Scanner

The Heidelberg Laser Tomographic Scanner (LTS) used a helium neon laser beam focused onto the fundus[43]. Images with sizes up to 20 by 20 degrees were obtained by scanning the structure point wise, line by line, in the given focal plane. In the case of optic disc recording, the first focal plane was defined directly above the first reflections of the retina. The last focal plane was selected in the region of the bottom of the excavation below the position of

maximum reflectivity of the excavation. Within the preselected focal planes, the LTS automatically completed an optic disc scan of 32 consecutive focal plane sections from the preretinal plane to the bottom of the excavation[43]. Given the optical quality of the human eye, the depth resolution was 300 μm. Automatic compilation of an optic disc scan of 32 consecutive focal plane sections is done in about 4 seconds.

Compared to the ONH analyzers, improved axial resolution and reduced variability in assessing optic nerve topography is improved with confocal scanning laser ophthalmoscopes, which produce optical sections of the retina and the ONH in a coronal plane. Cross-sectional imaging of the fundus with scanning laser ophthalmoscopes and tomographs is limited by ocular aberrations and numerical aperture available through pupil to 300 μm axial resolution. A major disadvantage of CSLO ONH measurements is that a reference plane is required to measure and calculate many of the parameters. The current software of the HRT defines the "standard reference plane" as a plane 50μm posterior to the mean height of the peripapillary retinal height along the contour line at a temporal segment between 350° and 356° below the horizontal line. Therefore the reference plane may change over time and give inaccurate data, especially in those with glaucoma who have changing topography[44]. Parameters that are independent of the reference plane include cup shape, cup volume below the surface, mean cup depth, maximum cup depth, and disc area.

ONH analyzers developed to quantitate cupping can measure rim area and provide indices of structure, but cannot as yet differentiate between normal and glaucomatous nerve heads and can only make limited efforts to detect changes over time.

NERVE FIBRE LAYER ANALYSIS

Studies of the NFL, rather than the optic nerve, should be used to detect the earliest signs of glaucomatous damage. Quigley and co-workers showed that change in retinal thickness due to NFL thinning secondary to ganglion cell death is a sensitive indicator of glaucomatous damage and may precede detectable changes in ONH appearance (cupping) and measurable loss of visual functions[45-47]. A reduction in thickness of only 10 to 20 μm may be significant, indicating impending visual field loss[45]. In fact, it is ganglion cell death that produces visual loss in glaucoma, and changes in the ONH only reflect the atrophy of the ganglion cells.

The nerve fiber analyzer

The NFL has birefringent properties: back and forth travel of light through it, causes a change of polarization known as retardance. Polarized light propagating through the retina is assumed to be rotated by the NFL in proportion to its thickness, therefore, measurements of the polarization state of reflected light provide information on NFL thickness. NFL thickness can be evaluated by measuring the retardance using Fourier ellipsometry[48].

Scanning laser ophthalmoscope

The high visibility of the NFL resulting from the high contrast imaging inherent in the confocal laser scanning configuration can be further enhanced using digital image enhancement techniques[49,50]. The confocal microscope can image NFL striations with high contrast and high lateral resolution and is not as dependent on pupil dilation or clear media as traditional photographic techniques[51]. The NFL striations are enhanced in this approach using digital filtering and polarization differential contrast imaging, in which changes in NFL appearance due to NFL birefringence are evaluated using two images obtained simultaneously with

orthogonal polarization[52].

Scanning laser polarimetry

Scanning laser polarimetry (NFA, NFA II, GDx) is a method of measuring the retinal nerve fiber layer thickness by use of a 780 nm near infrared diode polarized light. The double-passed reflected light is detected and analyzed in digital form and after adjacent scans are achieved, displayed in the form of a 256 × 256 pixel representing individual retinal positions covering 15°. The value of each pixel represents the amount of retardation – qualitatively yellow and white for high retardances while those that are dark blue represent low retardation. The time to acquire these 65,536 data locations is approximately 0.7 seconds. Measurements are obtained from a circular band of 1.5 to 2.5 disc diameters concentric to the disc. During the time of measurement, a compensation device neutralizes the corneal birefringence (but not the lenticular birefringence) to maximize polarization measurements of the retina[54].

An advantage of the scanning laser polarimeter is that it does not require pupil dilation. The polarimeter seems to be unaffected by both contact lens wear from ±4.0 dioptres to -8.5 dioptres and excimer laser treatment of corneas for moderate myopia. One disadvantage of the polarimeter is that the cornea and lens are polarizing structures that may alter the retardance, even with the use of the corneal compensator. In addition, retardance is a relative value and does not produce absolute NFL thickness values, unlike HRT and OCT measurements.

RETINAL THICKNESS MAPPING

Retinal thickness mapping with the Retinal Thickness Analyzer (RTA) is based on the principle of slit-lamp biomicroscopy in which a green 540nm HeNe laser is projected on the fundus at an angle and its intersection with the retina is imaged. The distance between the

intersection with the vitreo-retinal interface and that with the retina-retinal pigment epithelial interface is directly proportional to the retinal thickness. In about 400ms, a 2 × 2 mm area of the fundus is scanned, yielding 10 optical cross sections that are digitally recorded and an algorithm detects points grossly deviating from their neighbours. Unlike OCT, which yields individual optic sections, the retinal thickness mapping is capable of rapidly covering the macular area and its location relative to the fovea. The RTA is limited by pupil size and it is difficult to image those eyes with numerous floaters or media opacities such as advanced cortical cataracts[53].

CONFOCAL TOMOGRAPHIC ANGIOGRAPHY

This system combines the confocal laser scanner and Indocyanine green to visualize the vascular pattern of the deeper portions of the ONH, including the lamina cribrosa. Studies have proved that confocal tomographic angiography of patients with glaucomatous eyes had good correlation with their visual field defect location[54].

NEW OBJECTIVE FUNCTIONAL TESTS

All of the prior technologies to image the optic disc and NFL in glaucoma have been based on structural testing. Perimetry is a functional test that correlated well with structural assessments but is a subjective test that may not be able to detect early glaucomatous changes. Other functional tests showing promises are the pattern electroretinography (PERG) and multifocal electroretinography (MFERG)[54].

VISUAL FIELD ANALYSIS – HUMPHREY FIELD

ANALYZER

Two steps are involved in diagnosing glaucomatous visual field loss using automated perimetry. The first is to determine whether or not the visual field is normal. If the visual field is abnormal, the second step is to decide if the visual field abnormality is due to glaucoma or something else. When applied to perimetry, the term normal actually describes the range of test results found in the non diseased population. The range of normal has been determined experimentally, and the results are stored in the computer memory of the automated perimeter. If all statistical parameters are within the normal range, chances are that the visual field is normal. The sensitivity of automated threshold perimetry for detecting visual field defects is very high. But the specificity of automated perimetry is often not as high as clinicians would like. When performing perimetry on patients believed to have glaucoma, it is important to distinguish the visual field that appears abnormal because of artefacts from the visual field that are truly abnormal as a result of glaucoma or some other disease such as cataract, retinal disease, or neurologic lesions[55].

RELIABILITY INDICES

Reliability is tested by presenting “catch trial” targets designed to measure fixation losses, false-positive responses, and false-negative responses. The fixation loss rate relates to the number of times a patient responds to a target placed in the blind spot. If the fixation loss rate exceeds 20%, it is flagged. The false-positive error rate refers to the number of times a

patient responds to the audible click of the perimeter's shutter when no target is presented. The false-negative error rate refers to the number of times a patient fails to respond to a supra threshold (very bright) target placed in a seeing area of the visual field. The false-positive and false-negative errors are flagged if either exceeds 33%. The reliability indices are indicators of the extent to which a particular patient's results may be reliable compared with the normal range of value stored in the computer memory[56-58].

The patient's visual sensitivity for the fovea appears immediately below the reliability indices, along with any symbols denoting if foveal threshold fall beyond the normal 5%, 2%, 1% or 0.5% probability levels. The patient's visual sensitivity at each field location is presented below and to the right of the foveal sensitivity, with numeric values on the left and a graphic grey scale representation on the right. The numeric display gives the sensitivity of the visual field in decibels, with higher numbers denoting greater sensitivity. Decibels are a logarithmically based scale (10dB = 1 log unit) and represent units of attenuation of the highest luminance stimulus that the perimeter can present[55].

GREY SCALE

The grey scale indicates areas of high sensitivity with light shading and progressively lower sensitivities with darker shadings and so provides the reader with an overview of the pattern of visual field sensitivity. Given that this representation is based upon sampling locations within the visual field, the grey scale "fills in" areas between these tested locations by interpolation[55].

GLOBAL INDICES

The four global indices are found in the lower right hand corner of the printout. The

mean deviation (MD) is a measure of the average departure of each test location from the age-corrected normal value. The pattern standard deviation (PSD) is the standard deviation of the differences between the threshold value at each test location and the expected value. It is a measure of the extent to which the threshold determinations differ from each other. The short term fluctuation (SF) represents the variability of the patient's responses during the test. The corrected pattern standard deviation (CPSD) is similar to the PSD but is adjusted downward by subtracting that portion of the PSD which is actually caused by the SF. The calculation of global indices is weighted to give greater importance to the test locations near fixation and less importance to more peripheral locations[58-60].

If a global index is outside the expected normal range, a "p" value will appear next to it. The p value represents the proportion of normal subjects in which an index of that value is found. For example, if p<1% appears next to MD, fewer than 1% of normal subjects of that age will have an MD at that level. Any global index with a p value less than 5% has a high probability of being abnormal.

The MD is mainly an index of the size of a visual field defect. The MD is very sensitive to generalized loss of sensitivity, but purely localized defects that are large enough will also affect the MD.

The CPSD is an index of localized non uniformity of the surface of the hill of vision. It is extremely sensitive to localized visual field defects and is not at all affected by purely generalized loss of sensitivity. By looking at the MD and the CPSD, it is possible to anticipate the nature of any visual field defect before inspecting the rest of the data.

Table 1: Interpretation of the global indices on the Humphrey visual field analyzer

MD	CPSD	Interpretation
Normal	Normal	Visual field probably normal
Abnormal	Normal	Generalized loss of sensitivity
Normal	Abnormal	Small localized defect
Abnormal	Abnormal	Large defect with a significant localized component

TOTAL AND PATTERN DEVIATION

The total and pattern deviations are arrays of numbers and graphic plots in the centre and lower portions of the printout. The total deviation represents the difference between the measured threshold of each individual test location and the age-corrected normal value for that location. Visual field thresholds decline with age at the rate of between 0.5 to 1.0 decibels per decade. The pattern deviation represents the difference between an adjusted threshold of each individual test location and the age-corrected normal value for that location. The pattern deviation is derived from the total deviation by adjusting the measured threshold upward or downward by an amount that reflects any generalized change in the threshold of the least damaged portion of the visual field.

The graphic probability plots indicate how frequently a total or pattern deviation value at a particular test location will be found in the normal population. There are four symbols ranging from $p<5\%$ $p<0.5\%$[55].

GLAUCOMA HEMIFIELD TEST

The Glaucoma Hemifield test attempts to provide information about the difference

between the superior and inferior halves of the visual field[61,62]. The test evaluates the differences in threshold of mirror image groups of points on either side of the horizontal midline. There are five interpretive messages that may appear depending on the relationship of the thresholds in the superior and inferior halves of the field.

1. Within Normal Limits means that there is no significant difference between the superior and inferior halves of the fields and the overall sensitivity is within the 99.5% range of normal.
2. Outside Normal Limits appears when the threshold differences between the groups of points compared in the superior and inferior halves of the field are greater than would be expected in 99% of the normal population.
3. Borderline appears when the threshold differences are greater than would be expected in 97% of the normal population but not as great as in outside normal limits.
4. General reduction of sensitivity appears when the overall sensitivity of the least damaged portion of the visual field is depressed below the 99.5% range of normal, but there is no significant difference between the superior and inferior halves of the field.
5. Abnormally High sensitivity appears when the overall sensitivity is higher than expected in 99.5% of the normal population. This message is found most often in the presence of a high false-positive rate and usually represents an artifact of testing.

The specificity and sensitivity of the Glaucoma Hemifield Test for detecting nerve fiber bundle visual field defects are quite high.

CHOICE OF TEST PROGRAM

The standard test program used in glaucoma patients is the 30-2. The 24-2 eliminates the

peripheral test locations of the 30-2 program except for the most nasal portion of the field. The 10-2 program is useful in patients with very advanced field loss who only have a small island of vision persisting near fixation. The foveal sensitivity is also a very useful piece of information and should be turned on when performing threshold perimetry in glaucoma patients. Either the full threshold or full threshold from prior data strategies should be used when performing perimetry on the Humphrey Visual Field Analyzer[55].

NATURE OF GLAUCOMATOUS VISUAL FIELD DEFECTS

Never fiber bundle defects

Most visual field defects seen in glaucoma are of the nerve fiber bundle type[63]. Glaucoma causes loss of retinal fiber bundles by damaging ganglion cell axons at the optic nerve head. This loss may be either diffuse, localized, or both. The characteristic shape and location of the visual field defects seen in glaucoma result from the anatomy of the retinal nerve fiber layer[64]. The most characteristic feature of the nerve fiber bundle visual defect is the tendency to respect the horizontal meridian, especially of the nasal portion of the field. Isolated nerve fiber bundle defects rarely cross the nasal horizontal midline and typically end there abruptly. Even in patients with more advanced visual loss due to glaucoma, a detectable difference in the measured threshold on either side of the nasal horizontal midline often occurs.

Another feature of nerve fiber bundle visual field defects is the tendency to be found in the Bjerrum area which is between 10° and 20° from fixation temporally but fans out to between 2° to 25° nasally. Scotomas in this area often assume an arcuate shape with the circumferential diameter greater than the radial diameter. Fixation itself is usually spared unless the defect is far advanced. Nerve fiber bundle defects may, however, come to within 1° of

fixation.

Clinically, nerve fiber bundle defects may appear as paracentral or arcuate scotomas, nasal steps, temporal sector defects, or various combinations. Generalized loss of retinal sensitivity, enlargement of the blind spot, and selective loss of sensitivity in the nasal periphery without specific nerve fiber bundle characteristics have been described in glaucoma. There are many other causes for these types of visual field defects. Although any of them may occur as an isolated finding in glaucoma, more commonly they are associated with a nerve fiber bundle defect.

ARTIFACTS THAT MAY RESEMBLE VISUAL FIELD DEFECTS

Many artifacts of visual field testing can produce results resembling true visual field defects. An artifact does not reflect abnormal visual function. Rather, it results from the way the patient responds to the testing situation. Generalized depressions such as those seen in patients with cataracts or small pupils are not artifacts. They are true visual field defects that reflect diminished visual function. The learning effect is a common artifact in patients undergoing their first visual field examination. It typically appears as a loss of sensitivity which is more pronounced in the more peripheral portions of the field. The defect either disappears or markedly improves after the second or third examination. An apparent depression in the superior peripheral portion of the field may resemble an arcuate scotoma in the grey scale. The superior portion of the visual field normally has lower sensitivity and higher variability. Even mild blepharoptosis may produce significant depressions in the superior visual field resembling the defects seen in glaucoma. To obtain accurate central visual fields, the patient’s refractive correction must be placed in the perimeter. In general, about one decibel of loss will appear for

each dioptre of over or under correction placed in the perimeter. If the pupil is smaller than 2.5 mm, an otherwise normal visual field may appear to be depressed, whereas an abnormal visual field may appear worse than it really is[65]. The pupil size should be recorded each time the visual field is tested. Fatigue and an unduly long examination time may also be associated with depressed sensitivity and apparent visual field defects[66].

In conclusion, automated perimetry is an extremely useful tool and has become the standard technique for evaluating the visual field in patients with or believed to have glaucoma. Interpretation of the results is difficult and requires experience as well as a detailed understanding of the underlying principles of automated static perimetry and applied statistical analysis.

AIMS AND OBJECTIVES

8. To analyze and establish the structure functional relationship between OCT macular volume /thickness parameters in patients with POAG SUSPECTS and POAG CASES .

9. To correlate macular thickness and RNFL thickness in primary open angle glaucoma suspects and primary open angle glaucoma patients using OPTICAL COHERENCE TOMOGRAPHY (OCT).

ETHICS

Informed consent of patients is taken in all cases analyzed clinically after explaining the nature of tests, its cost , clinical benefits and need for a follow up if necessary for analysis of progression of glaucoma .

Approval is obtained by the hospital ethical committee .

MATERIALS AND METHODS

A prospective study to analyze and establish the structure functional relationship between OCT macular volume/thickness parameters in patients with POAG –SUSPECTS and POAG PATIENTS was undertaken in the department of glaucoma services , ARAVIND EYE HOSPITAL , MADURAI .

The study was conducted between November 2004 and September 2005, during which period a total of 290 eyes of 146 patients were studied and analyzed.

SUBJECTS

INCLUSION CRITERIA

- Patients in the age group of 14 -75 years.
- Patients with suspected POAG and patients with POAG diagnosed at the time of study or previously diagnosed as POAG patient.
- Open angles on gonioscopy using modified shaffer's grading system.
- Patients with refractive errors-myopia less than 5 diopters , hypermetropia less than 3.5 diopters and astigmatism less than 2 diopters.
- Patients who were cooperative and willing for the study were included in the study.

EXCLUSION CRITERIA

4. Patients outside the age group specified in the inclusion criteria.
5. All types of glaucoma other than POAG.
6. All gross media opacities which interfere with the OCT imaging.
7. Patients with retinal and macular diseases.

CLASSIFICATION CRITERIA

POAG SUSPECT

6. No history of glaucoma
7. BCVA 20/40 OR better.
8. IOP ≤ 21mm Hg.
9. HFA normal / subtle defects.
10. Abnormal /Asymmetrical cupping of the optic nerve head .

POAG

- Incomplete NRR loss in any 1 quadrant /quadrantic NRR loss .
- Visual field loss one side of the horizontal meridian by HFA / Visual field loss above and below the horizontal meridian.
- IOP > 21mm Hg.

All patients had full ophthalmic evaluation including refraction, slit lamp examination, gonioscopy, goldmann applanation tonometry, dilated stereoscopic fundus examination , visual field testing and prototype –STRATUS OCT SCANNING (OCT 3) .

Patients pupils were dilated with 1% tropicamide and 2.5% phenylephrine hydrochloride before recording the images .Each subject had circular scans around the optic nerve head as possible without overlapping the disc itself. This gives approximately 500 and 750 microns of offset from the edge of the optic nerve head respectively. 2 radial scans were performed one from 12 to 6 0clock position and another from 3 to 9 oclock position, through the centre of the optic nerve head.

The examiner centered the circular or radial scan on the optic nerve head while the

subject fixates on an internal fixation light shone in the eye being scanned that could be offset from the scan .The offset information in transverse direction between the fixation light and the scan pattern was recorded for automatic registration of subsequent scans .The scans were performed using near infra red illumination 840 nanometres to minimize subject discomfort.

Macular thickness measurements were generated using 6 radial scans each 5.9 millimetres centered on the fovea. These scans were processed to produce a topographic map of the macula. Mean quadrantic measurements were generated from the retinal map consisting of sectoral measurements located 0.5 mm to 1.7 mm outside the centre of the fovea.

OCT macular neurosensory retinal thickness maps were used to calculate macular volume /thickness for comparision to humphrey visual field testing, intraocular pressure (IOP) measurements, optic nerve head damage and nerve fibre layer thickness.

Orthogonal OCT macular analysis was obtained to maximize the sampling of the area of interest .Area under the receiver operator characteristics (AROC) curves for the association between macular retinal thickness and peripapillary NFL thickness and visual field findings were calculated in a sub group of eyes without visual field defect and eyes with visual field defect confined to one hemifield .

STATISTICAL ANALYSIS

The data were analyzed using strata 8.1 software (STATA CORPORATION ,COLLEGE STATION ,TEXAS ,USA). Mann Whitney U test were calculated for non parametric data and area under receiver operator characteristic (AROC) curves were calculated for the association between visual field defects confined to a single hemifield and macular and peripapillary hemiretinal OCT measurements.

PROFORMA

A prospective analysis of Macular volume and thickness parameters in Primary open angle glaucoma suspects and patients with Primary open angle glaucoma by OCT

Case No : ----------

M.R. No : ----------

Date : ----------

Patient Particulars

Name : ----------

Age : ----------

Sex : ----------

Occupation : ----------

Address : ----------

Patient examination

BCVA RE _____

LE _____

IOP RE _____

LE _____

Gonioscopy RE ☒

LE ☒

Slit lamp biomicroscopy with 90D lens

Intra papillary changes	RE	LE
Disc size		
Disc shape		
Cup : Disc ratio		
Para papillary changes		
RNFL		
NRR loss		
Macula		

Visual field by HFA analysis

Visual field loss	RE	LE
Either side of Horizontal meridian		
Both sides of Horizontal meridian		
Global Indices		
Mean Deviation		
Pattern Standard deviation		

MACULAR THICKNESS AND VOLUME SCAN

Name :---------- M.R. No ---------- Diagnosis ----------

		OD	OS	DIFF

Average Retinal thickness (μm)	Fovea minimum Fovea			
	Temporal inner macula			
	Superior inner macula			
	Nasal inner macula			
	Inferior inner macula			
	Temporal Outer macula			
	Superior Outer macula			
	Nasal Outer macula			
	Inferior Outer macula			
Ratio	Superior / inferior outer			
	Temporal / nasal inner			
Volu	Temporal / nasal outer			
me (cubic mm)	Fovea			
	Temporal inner macula			
	Superior inner macula			
	Nasal inner macula			
	Inferior inner macula			
	Temporal Outer macula			
	Superior Outer macula			
	Nasal Outer macula			
	Inferior Outer macula			
	Total macula volume			

O.D.

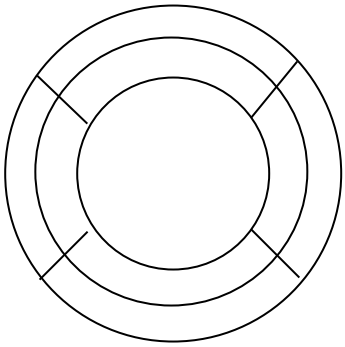

O.S.

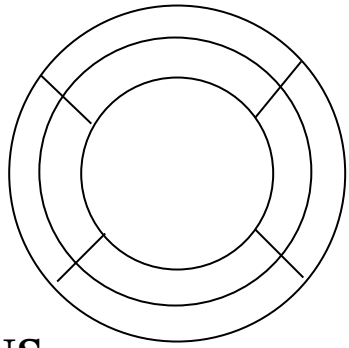

OBSERVATIONS

About The Receiver Operating Characteristic curve

Sensitivity and specificity are the basic measures of accuracy of a diagnostic test. They describe the abilities of a test to enable one to correctly diagnose disease when disease is

actually present and to correctly rule out disease when it is truly absent.

However, they depend on the cut point used to define “positive” and “negative” test results. As the cut point shifts, sensitivity and specificity shifts. The receiver operating characteristic (ROC) curve is a plot of the sensitivity of a test (plotted on the y-axis) versus its false-positive rate (1-specificity, plotted on the x-axis) for all possible cut points.

The accuracy of a test is measured by comparing the results of the test to the true disease status of the patient. The true disease status is determined with the reference standard procedure[67].

The ROC curve area is a good summary measure of test accuracy because it does not depend on the prevalence of the disease or the cut points used to form the curve. The ROC curve has been used to assess the test accuracy of OCT and Visual Fields in diagnosing Glaucoma.

An ROC curve demonstrates several things:

10. It shows the cutoff between sensitivity and specificity (any increase in sensitivity will be accompanied by a decrease in specificity).
11. The closer the curve follows the left-hand border and then the top border of the ROC space, the more accurate the test.
12. The closer the curve comes to the 45-degree diagonal of the ROC space, the less accurate the test.
13. The slope of the tangent line at a cut point gives the likelihood ratio (LR) for that value of the test.

14. The area under the curve (AUC) is a measure of test accuracy.

OBSERVATIONS

	OCT Region	AROC superior	AROC Inferior	p-value
Sup. VF defect	Macula	0.66	0.72	0.006
(N = 112)	Peripapillary NFL	0.74	0.75	0.621
Inf. VF defect	Macula	0.69	0.73	0.116
(N = 101)	Peripapillary NFL	0.70	0.71	0.660
Inf = inferior; NFL = nerve fiber layer; Sup = superior; VF = visual field				

This table gives the AROC values of macular and peripapillary NFL thickness in areas corresponding to the VF defect location.

In eyes with superior VF defect, the AROC value was significantly higher in the inferior retina for both macular and peripapillary NFL measurement and more significant for peripapillary NFL thickness than macular thickness. While in eyes with inferior VF defect the AROC value was not of much significance.

Macular Retinal and Peripapillary NFL Hemiretinal Thickness (Mean ± SD) in Subjects with no VF Defect or a Defect Confined to a Single Hemifield

	Macular Retinal Thickness µm (SD)			**Peripapillary NFL Thickness µm (SD)**		
VF Defect Location	Superior	Inferior	p-value	Superior	Inferior	p-value
None (N = 121)	251.2 (15.2)	250.7 (31.6)	NA	148.1 (21.9)	156.5 (27.1)	NA
Superior (N= 68)	245.6 (18.7)	240.3 (15.3)	0.087	132.1 (23.7)	136.2 (26.3)	0.400
Inferior (N = 57)	244.4 (15.0)	240.0 (14.2)	0.439	135.9 (27.8)	140.6 (26.8)	0.322
Both (N = 44)	224.7 (21.7)	214.3 (18.7)	0.059	100.5 (28.1)	97.4 (30.6)	0.026

NA = not applicable; NFL = nerve fiber layer; Sup = superior; VF = visual field

This table compares the areas of VF defect with the macular thickness and peripapillary thickness. Patient's with no VF defect showed not much difference in the thickness.

Patient's with superior VF defect showed a corresponding thinning in the inferior macular thickness but not in peripapillary NFL thickness.

Patient's with inferior VF defect showed a corresponding thinning in the superior macular thickness but not in the peripapillary NFL thickness.

Patient's with both superior and inferior VF defect showed a corresponding thinning in both superior and inferior macular thickness as well in the peripapillary NFL thickness.

Comparison of Study Population Characteristics (Mean ± SD)

	No VF Defect	Single Hemifield VF Defect	Both Hemifield VF Defect	ANOVA
Eyes	121	125	44	NA
Age (yr)	46.40 (12.2)	52.29 (11.8)	51.26 (13.3)	0.028
MD (dB)	-1.93 (4.72)	-5.15 (4.41)	-13.66 (11.26)	0.000
PSD (dB)	3.52 (2.11)	4.25 (2.46)	6.19 (4.30)	0.000

ANOVA – analysis of variance; MD – mean deviations; PSD – pattern standard deviation; VF – visual field; NA – not applicable

This table shows the characteristics of the study population. The difference in mean age among the 3 groups was significant. Patient's with no VF defect were younger than those with a single or both hemifield VF defect.

AROC CURVES

To evaluate the association between macular retinal and peripapillary NFL thickness with VF defect, AROC curves were calculated.

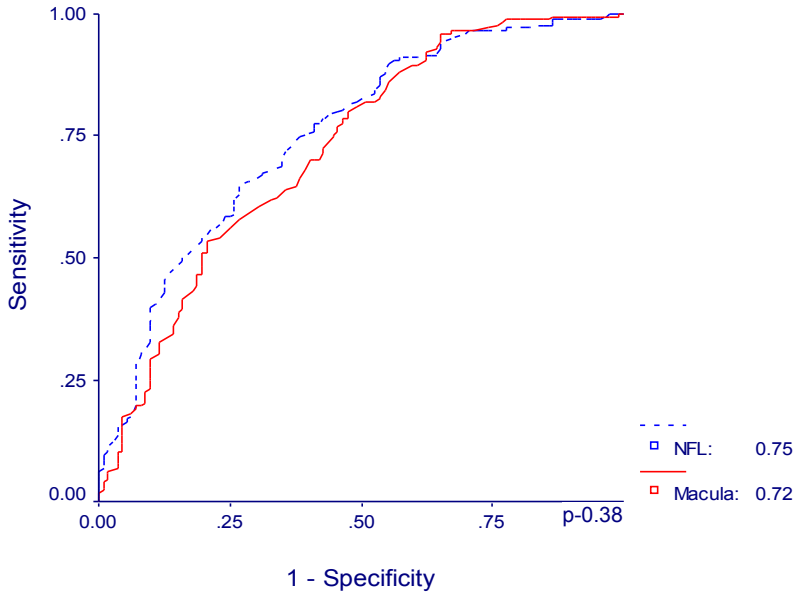

Area under the receiver operating characteristic (AROC) curves for optical coherence tomography inferior macular retinal and peripapillary (NFL) measurements for eyes with visual defects confined to the superior hemifield.

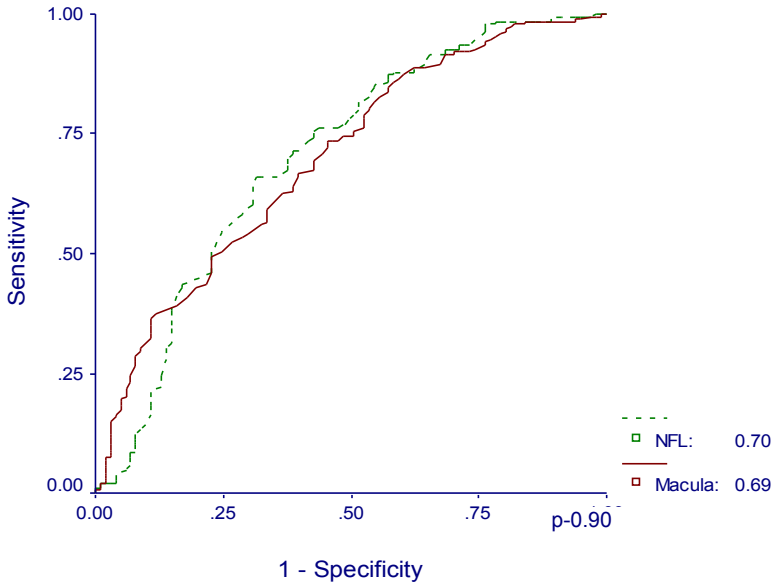

Area under the receiver operating characteristic (AROC) curves for optical coherence tomography superior macular retinal and peripapillary (NFL) measurements for eyes with visual defects confined to the inferior hemifield.

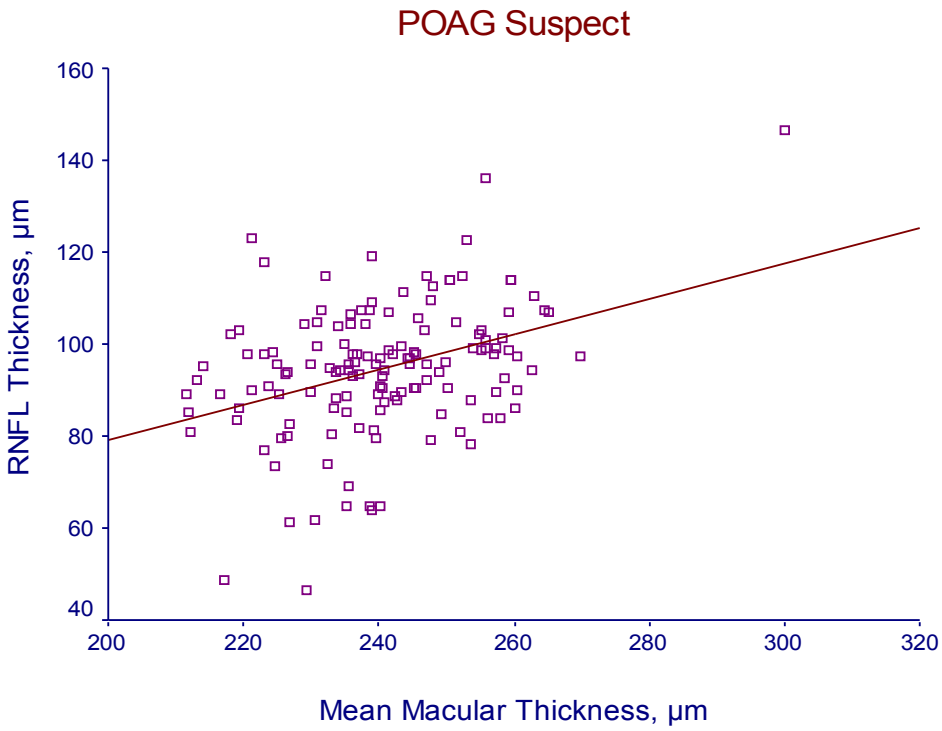

This Scatter diagram illustrates the correlation between mean macular thickness and peripapillary retinal nerve fiber layer (RNFL) thickness (r=0.373; p=0.000). Hence the mean macular thickness is significantly associated with mean RNFL thickness in POAG suspect.

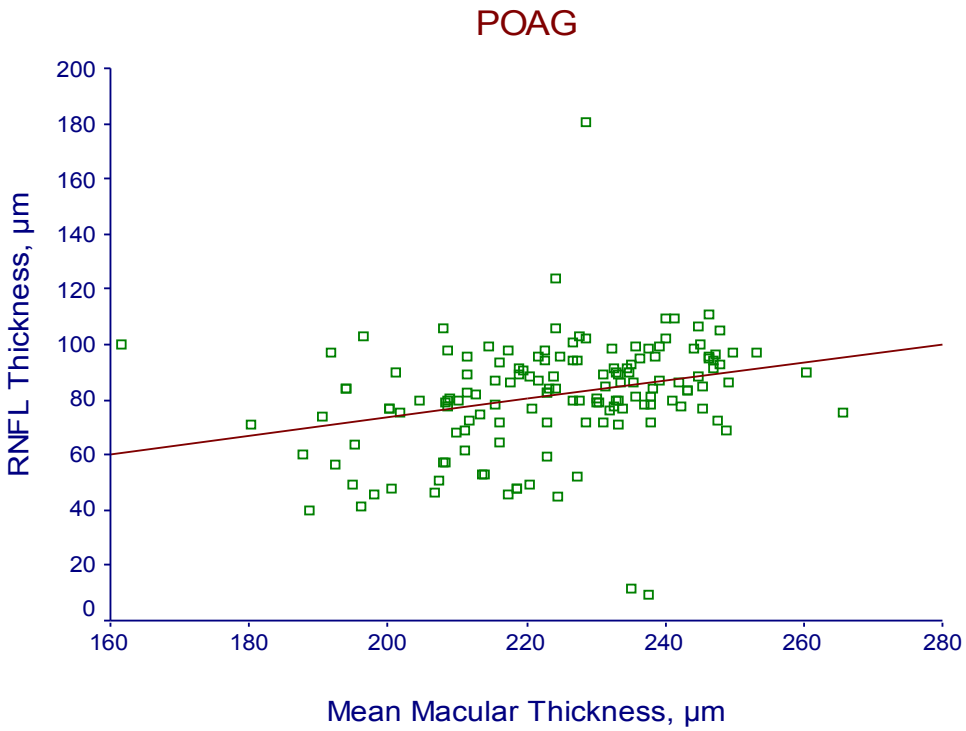

This Scatter diagram illustrates the correlation between mean macular thickness and peripapillary retinal nerve fiber layer (RNFL) thickness (r=0.291; p=0.000). Hence the mean macular thickness is significantly associated with mean RNFL thickness in POAG.

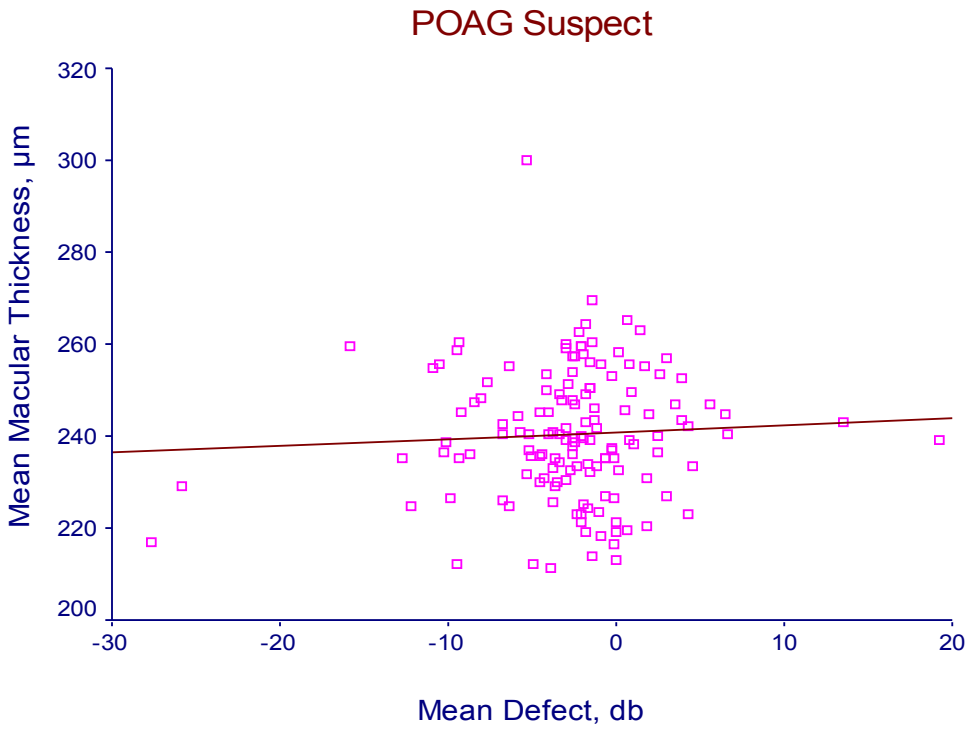

This Scatter diagram illustrates the correlation between visual field mean defect and macular thickness ($r = 0.056$; $p=0.505$) is not found to be significant in POAG suspect.

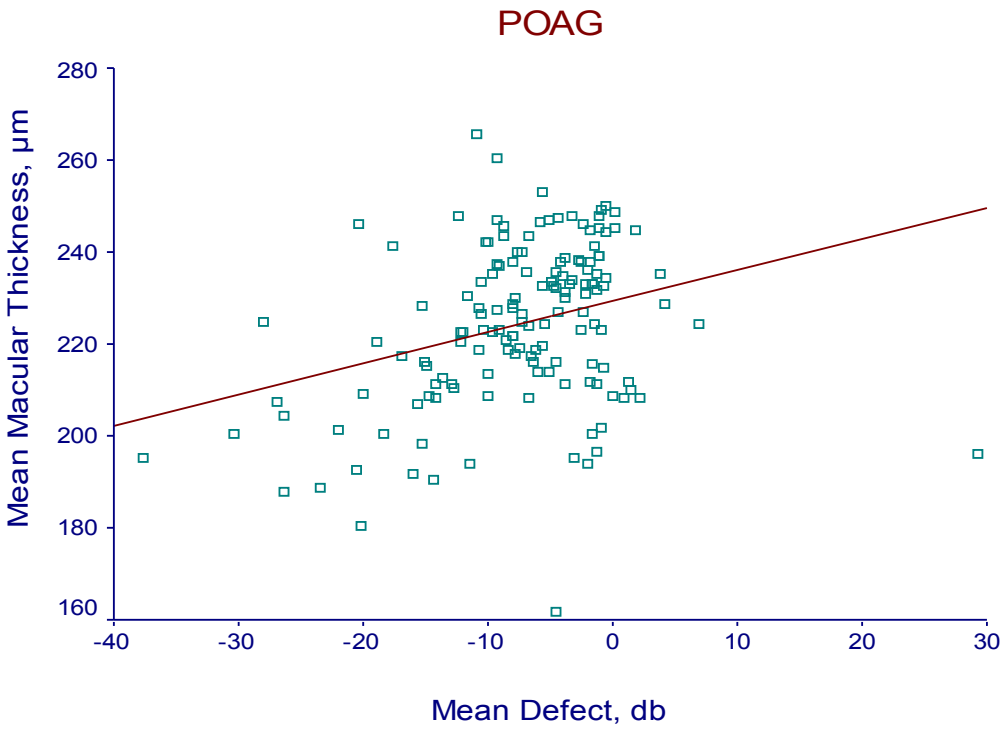

This Scatter diagram illustrates the correlation between visual field mean defect and macular thickness ($r = 0.305$; $p=0.000$) is found to be significant in POAG.

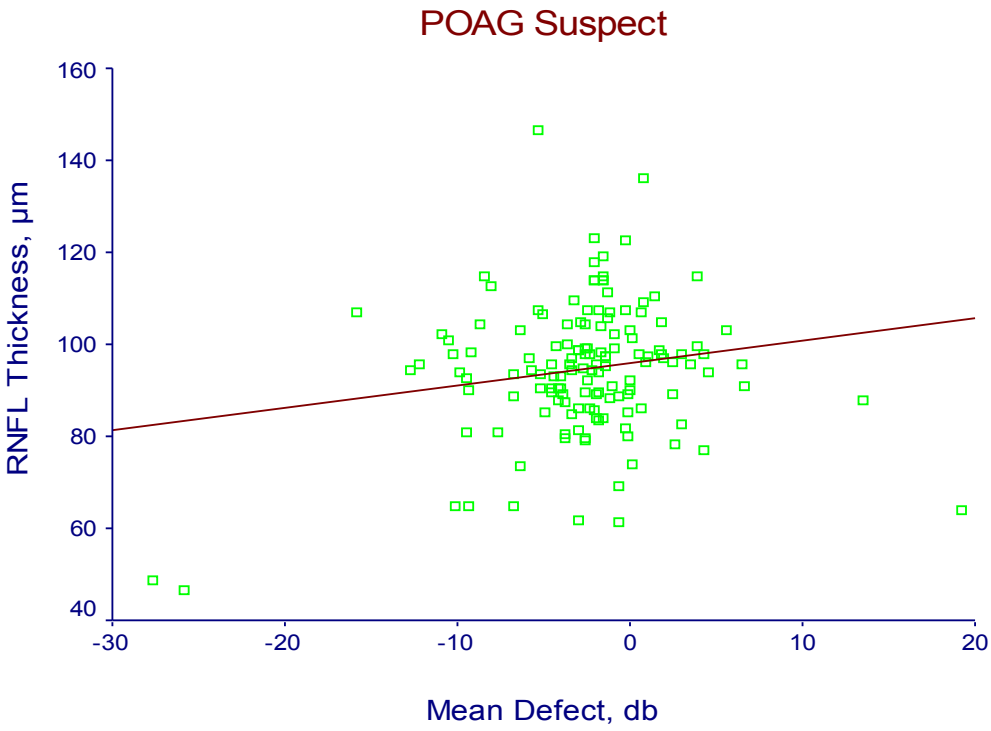

This Scatter diagram illustrates the correlation between visual field mean defect and peripapillary retinal nerve fiber layer (RNFL) thickness (r = 0.181; p=0.031) is found to be significant in POAG suspects.

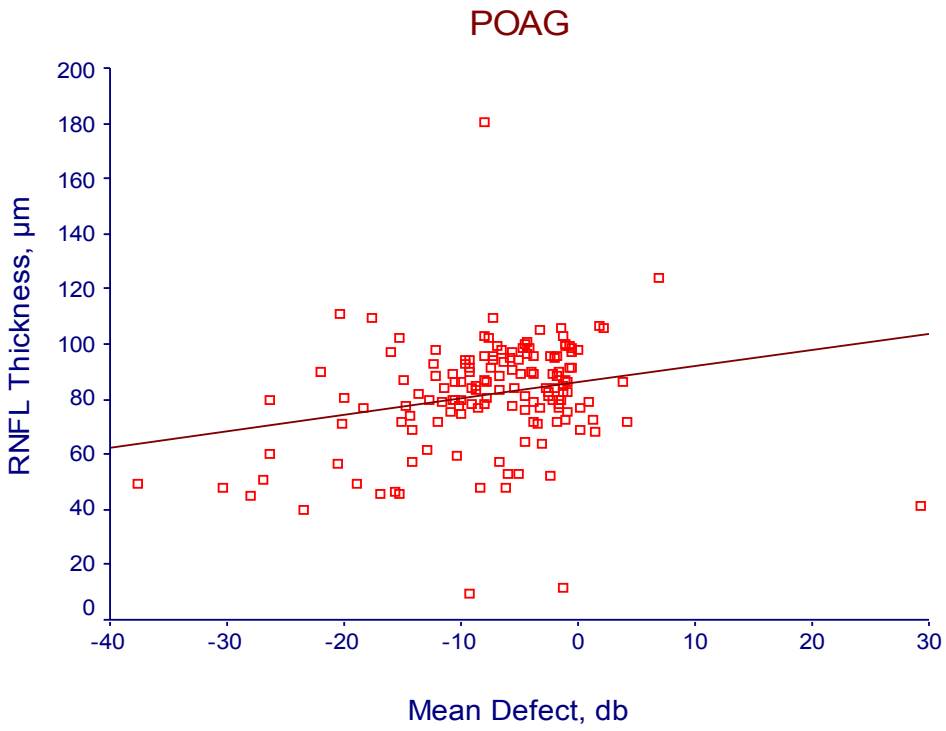

This Scatter diagram illustrates the correlation between visual field mean defect and peripapillary retinal nerve fiber layer (RNFL) thickness (r = 0.236; p=0.004) is found to be significant in POAG.

Descriptive Statistics (p-0.002) - Mann-Whitney U Test

Diagnosis		N	Minimum	Maximum	Mean	Std. Deviation
POAG Suspect	Age	69	14	73	46.68	12.244
POAG	Age	76	25	73	52.66	12.121

Sex Vs Diagnosis Crosstabulation (p-0.337) Pearson Chi-square test

			Diagnosis		
			POAG Suspect	POAG	Total
Sex	Male	Count	53	53	106
		% within Sex	50.0%	50.0%	100.0%
		% within Diagnosis	76.8%	69.7%	73.1%
	Female	Count	16	23	39
		% within Sex	41.0%	59.0%	100.0%
		% within Diagnosis	23.2%	30.3%	26.9%
Total		Count	69	76	145
		% within Sex	47.6%	52.4%	100.0%
		% within Diagnosis	100.0%	100.0%	100.0%

Descriptive Statistics (p - 0.585) - Mann - Whitney U Test

Diagnosis		N	Minimum	Maximum	Mean	Std. Deviation
POAG Suspect	IOP	142	8	30	18.36	4.439
POAG	IOP	148	9	37	18.22	4.748

Descriptive Statistics (p - 0.000) - Mann - Whitney U Test

Diagnosis		N	Minimum	Maximum	Mean	Std. Deviation
POAG Suspect	Mean	142	-27.72	19.26	-2.6480	5.35390
POAG	Mean	148	-37.60	29.22	-7.4548	7.94520

Descriptive Statistics (p - 0.171) - Mann - Whitney U Test

Diagnosis		N	Minimum	Maximum	Mean	Std. Deviation
POAG Suspect	Pattern Standard deviation	142	-3.77	12.51	3.8642	2.34099
POAG	Pattern Standard deviation	148	.02	16.53	4.6075	3.19756

Descriptive Statistics (p - 0.194) - Mann - Whitney U Test

Diagnosis		N	Minimum	Maximum	Mean	Std. Deviation
POAG Suspect	Foveal Minimum	142	107	466	167.52	36.143
POAG	Foveal Minimum	148	107	248	160.62	22.712

Descriptive Statistics (p - 0.000) - Mann - Whitney U Test

Diagnosis		N	Minimum	Maximum	Mean	Std. Deviation
POAG Suspect	Total Macular volume	142	5.897	12.166	6.83206	.581790
POAG	Total Macular volume	148	4.582	7.545	6.35303	.496317

Descriptive Statistics (p - 0.000) - Mann - Whitney U Test

Diagnosis		N	Minimum	Maximum	Mean	Std. Deviation
POAG Suspect	Average retinal thickness	142	46.50	146.35	94.5523	14.50736
POAG	Average retinal thickness	148	9.41	180.71	81.5808	20.13333

Descriptive Statistics (p - 0.000) - Mann - Whitney U Test

Diagnosis		N	Minimum	Maximum	Mean	Std. Deviation
POAG Suspect	SMAX	142	57.00	195.00	146.0493	24.01812
POAG	SMAX	148	49.00	188.00	123.9879	29.78971

Descriptive Statistics (p - 0.000) - Mann - Whitney U Test

Diagnosis		N	Minimum	Maximum	Mean	Std. Deviation
POAG Suspect	IMAX	142	62.00	232.00	153.7183	27.80488
POAG	IMAX	148	46.00	206.00	126.2086	33.58742

Descriptive Statistics (p - 0.007) - Mann - Whitney U Test

Diagnosis		N	Minimum	Maximum	Mean	Std. Deviation
POAG Suspect	Fovea	142	133	483	197.48	34.418
POAG	Fovea	148	133	267	187.43	20.809

Descriptive Statistics (p - 0.000) - Mann - Whitney U Test

Diagnosis		N	Minimum	Maximum	Mean	Std. Deviation
POAG Suspect	Temporal inner macula	142	198	379	256.52	21.120
POAG	Temporal inner macula	148	122	292	240.74	23.472

Descriptive Statistics (p - 0.000) - Mann - Whitney U Test

Diagnosis		N	Minimum	Maximum	Mean	Std. Deviation
POAG Suspect	Superior inner macula	142	208	369	267.39	21.446
POAG	Superior inner macula	148	177	308	254.03	21.005

Descriptive Statistics (p - 0.000) - Mann - Whitney U Test

Diagnosis		N	Minimum	Maximum	Mean	Std. Deviation
POAG Suspect	Nasal inner macula	142	211	606	273.08	33.913
POAG	Nasal inner macula	148	136	298	253.99	24.247

Descriptive Statistics (p - 0.000) - Mann - Whitney U Test

Diagnosis		N	Minimum	Maximum	Mean	Std. Deviation
POAG Suspect	Inferior inner macula	142	226	596	273.42	31.771
POAG	Inferior inner macula	148	186	302	253.59	22.474

Descriptive Statistics (p - 0.000) - Mann - Whitney U Test

Diagnosis		N	Minimum	Maximum	Mean	Std. Deviation
POAG Suspect	Temporal Outer macula	142	186	322	220.01	19.302
POAG	Temporal Outer macula	148	130	242	201.98	18.258

Descriptive Statistics (p - 0.000) - Mann - Whitney U Test

Diagnosis		N	Minimum	Maximum	Mean	Std. Deviation
POAG Suspect	Superior Outer macula	142	195	292	235.74	16.424
POAG	Superior Outer macula	148	141	271	221.76	20.573

Descriptive Statistics (p - 0.000) - Mann - Whitney U Test

Diagnosis		N	Minimum	Maximum	Mean	Std. Deviation
POAG Suspect	Nasal Outer macula	142	190	554	257.34	30.486
POAG	Nasal Outer macula	148	133	292	238.35	23.624

Descriptive Statistics (p - 0.000) - Mann - Whitney U Test

Diagnosis		N	Minimum	Maximum	Mean	Std. Deviation
POAG Suspect	Inferior Outer macula	142	191	509	227.48	28.721
POAG	Inferior Outer macula	148	109	277	209.08	20.246

Descriptive Statistics (p - 0.000) - Mann - Whitney U Test

Diagnosis		N	Minimum	Maximum	Mean	Std. Deviation
POAG Suspect	Inner ring	142	223.00	478.50	267.6021	24.36475
POAG	Inner ring	148	171.00	297.50	250.5878	20.78201

Descriptive Statistics (p - 0.000) - Mann - Whitney U Test

Diagnosis		N	Minimum	Maximum	Mean	Std. Deviation
POAG Suspect	Outer ring	142	206.50	413.50	235.1426	20.42517
POAG	Outer ring	148	159.50	258.75	217.7922	17.65713

Descriptive Statistics (p - 0.000) - Mann - Whitney U Test

Diagnosis		N	Minimum	Maximum	Mean	Std. Deviation
POAG Suspect	Center+inner	142	182.00	480.75	232.5405	27.62261
POAG	Center+inner	148	158.50	269.75	219.0101	18.05291

SUPINF Vs VF Defect Location (p-0.087) Mann-whitney U Test

	VF Defect Location	N	Mean	Std. Deviation	Std. Error Mean
SUPINF	None	121	.5207	25.74979	2.34089
	Superior	68	5.3015	12.50735	1.51674

SUPINF Vs VF Defect Location (p-0.439) Mann-whitney U Test

	VF Defect Location	N	Mean	Std. Deviation	Std. Error Mean
SUPINF	None	121	.5207	25.74979	2.34089
	Inferior	57	4.4035	11.78431	1.56087

SUPINF Vs VF Defect Location (p-0.059) Mann-whitney U Test

	VF Defect Location	N	Mean	Std. Deviation	Std. Error Mean
SUPINF	None	121	.5207	25.74979	2.34089
	Both	44	10.3295	23.15216	3.49032

SMAXIMAX Vs VF Defect Location (p-0.400) Mann-whitney U Test

	VF Defect Location	N	Mean	Std. Deviation	Std. Error Mean
SMAXIMAX	None	121	-8.3471	28.12286	2.55662
	Superior	68	-4.0656	22.97460	2.78608

SMAXIMAX Vs VF Defect Location (p-0.322) Mann-whitney U Test

	VF Defect Location	N	Mean	Std. Deviation	Std. Error Mean
SMAXIMAX	None	121	-8.3471	28.12286	2.55662
	Inferior	57	-4.6388	26.17579	3.46707

SMAXIMAX Vs VF Defect Location (p-0.026) Mann-whitney U Test

	VF Defect Location	N	Mean	Std. Deviation	Std. Error Mean
SMAXIMAX	None	121	-8.3471	28.12286	2.55662
	Both	44	3.0273	26.78624	4.03818

Descriptive Statistics

VF Defect Location		N	Mean	Std. Deviation
None	SUPERIOR	121	251.2686	15.23921
	INFERIOR	121	250.7479	31.67433
	SMAX	121	148.1653	21.92766
	IMAX	121	156.5124	27.19593
Superior	SUPERIOR	68	245.6471	18.73979
	INFERIOR	68	240.3456	15.36090
	SMAX	68	132.1815	23.76700
	IMAX	68	136.2471	26.35252
Inferior	SUPERIOR	57	244.4825	15.01843
	INFERIOR	57	240.0789	14.20506
	SMAX	57	135.9661	27.85781
	IMAX	57	140.6049	26.87916
Both	SUPERIOR	44	224.7045	21.77697
	INFERIOR	44	214.3750	18.78957
	SMAX	44	100.5182	28.19716
	IMAX	44	97.4909	30.68715

Descriptives

Age

	N	Mean	Std. Deviation	Std. Error	95% Confidence Interval for Mean		Minimum	Maximum
					Lower Bound	Upper Bound		
No VF Defect	57	46.40	12.297	1.629	43.14	49.67	14	73
Single Hemifield VF Defect	65	52.29	11.874	1.473	49.35	55.23	18	71
Both Hemifield VF Defect	23	51.26	13.322	2.778	45.50	57.02	26	73
Total	145	49.81	12.502	1.038	47.76	51.87	14	73

Descriptives

Mean

	N	Mean	Std. Deviation	Std. Error	95% Confidence Interval for Mean		Minimum	Maximum
					Lower Bound	Upper Bound		
No VF Defect	121	-1.9331	4.72029	.42912	-2.7828	-1.0835	-15.90	19.26
Single Hemifield VF Defect	125	-5.1522	4.41575	.39496	-5.9340	-4.3705	-20.30	3.89
Both Hemifield VF Defect	44	-13.6680	11.26855	1.69880	-17.0939	-10.2420	-37.60	29.22
Total	290	-5.1011	7.20333	.42299	-5.9337	-4.2686	-37.60	29.22

Descriptives

Pattern Standard deviation

	N	Mean	Std. Deviation	Std. Error	95% Confidence Interval for Mean		Minimum	Maximum
					Lower Bound	Upper Bound		
No VF Defect	121	3.5207	2.11420	.19220	3.1402	3.9013	-3.77	12.51
Single Hemifield VF Defect	125	4.2551	2.46086	.22011	3.8195	4.6908	.02	15.24
Both Hemifield VF Defect	44	6.1982	4.30550	.64908	4.8892	7.5072	.30	16.53
Total	290	4.2435	2.83072	.16623	3.9164	4.5707	-3.77	16.53

CD Ratio Vs Diagnosis (p-0.000) Mann-Whitney U Test

Diagnosis		N	Minimum	Maximum	Mean	Std. Deviation
POAG Suspect	CD Ratio	142	.3	.8	.633	.1253
POAG	CD Ratio	148	.3	.9	.690	.1048

VF Defect Location

	Frequency	Percent
No VF Defect	121	41.7
Single Hemifield VF Defect	125	43.1
Both Hemifield VF Defect	44	15.2
Total	290	100.0

Visual Field Defect Location

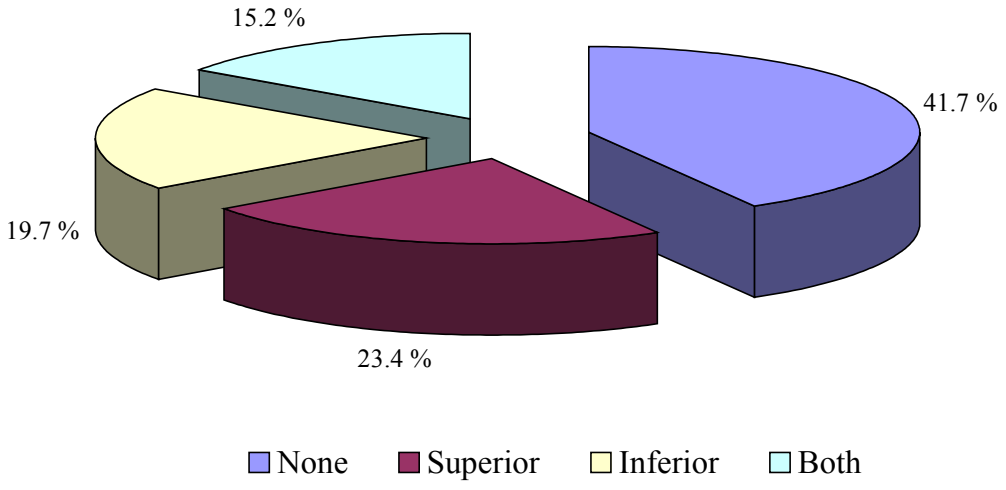

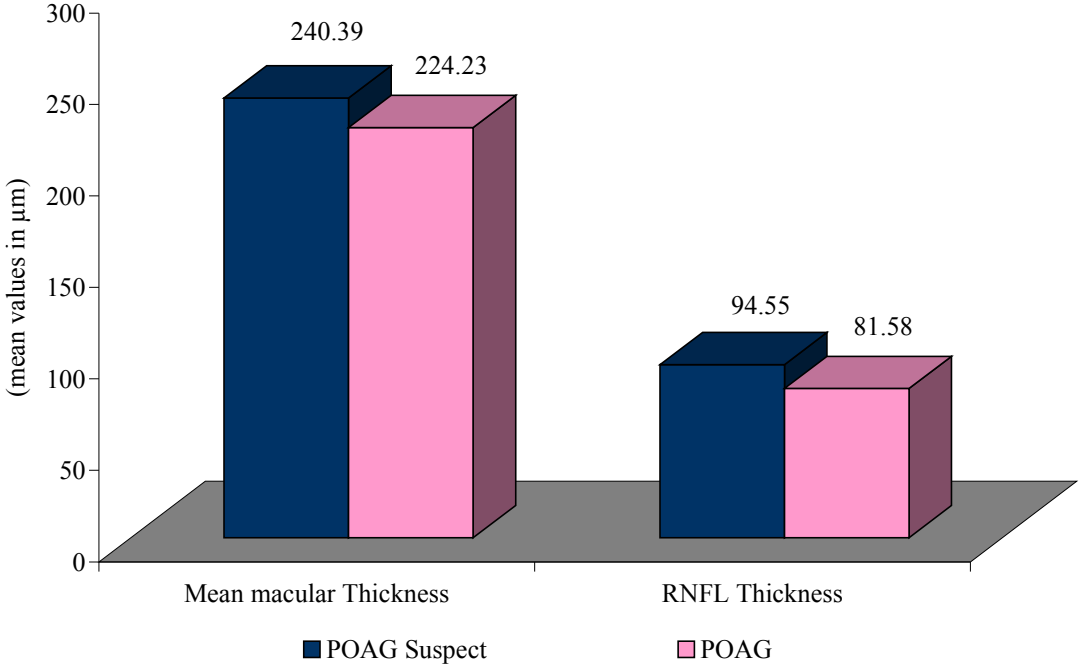

Diagnosis		N	Minimum	Maximum	Mean	Std. Deviation
POAG Suspect	Mean Macular thickness	142	211.40	300.00	240.39	14.0439
POAG	Mean Macular thickness	148	161.68	265.53	224.23	17.5551

The P value was found to be 0.000.

DISCUSSION

This study was designed with the objective of analyzing the macular thickness and volume parameters in primary open angle glaucoma suspects (POAG Suspects) and primary open angle glaucoma (POAG) patients and establish the structure functional relationship between OCT macular volume / thickness parameters in POAG Suspects and POAG patients.

The study also compared the macular thickness with RNFL thickness in its association with the disease and found that the macular thickness changes to be correlating well with changes in the retinal nerve fiber layer , hence represent a surrogate indicator of retinal ganglion cell loss .

A total of 290 eyes were studied , out of which 142 eyes were diagnosed as POAG Suspects and 148 eyes as POAG .The data was analyzed in a number of ways , most specifically comparing means between the groups and analyzing AROC ’s .We chose AROC ’s because it is a summary statistic for sensitivity and specificity . The disadvantage of the AROC is that it does not describe the shape of the curve , only the area underneath it , so the number alone does not define the relationship between the sensitivity and specificity for the given comparison .

Areas under the receiver operator characteristics for macular thickness and peripapillary NFL thickness were studied and were found to be higher in areas corresponding to the VF

defect location than the non corresponding locations .Higher AROC values were found for areas that correspond to the location of the VF defect .

In our study , eyes with superior VF defects , the AROC values was significantly higher in the inferior retina than the superior for both macular retinal and peripapillary NFL measurements .Eyes with inferior VF defects , the difference in AROC ’s for corresponding and non corresponding locations was not significant for macular retinal measurements but marginally significant for peripapillary NFL measurements . Comparing AROC ’s of macular and peripapillary NFL measurements at the same locations , the AROC for inferior peripapillary NFL was significantly higher compared to the inferior macular retinal measurements in patients with superior VF defects .

The RNFL thickness showed a slightly stronger relationship with the disease compared to the macular retinal thickness . But , this finding may be due to under sampling of the tissue at risk , because only approximately 50 % of the retinal ganglion cells are present in the macula , yet nearly 100 % of the retinal ganglion cells are assessed in a peripapillary OCT NFL scan . Since glaucoma is a diffuse disease , the ability to measure the damage done by glaucoma in the entire eye may give peripapillary NFL assessment a distinct advantage over macular thickness evaluation in detecting glaucoma .

Another major advantage of the RNFL measurement over macular thickness measurement is the confounding of macular thickness measures by non glaucomatous macular disease like diabetes and macular degenerations , directly affecting macular thickness and could

obscure or exaggerate the abnormalities seen with glaucoma . These are not significant issues in peripapillary NFL assessment .This is not to say that macular thickness measurement may not be a useful parameter in the evaluation of glaucoma . It is significantly associated with the disease , and there may be fewer technical challenges in its measurement than in the quantitation of peripapillary NFL thickness .

We found in this study that the OUTER RING macular thickness with our prototype OCT provided better correlation than did the INNER RING macular thickness in both the study groups . Thus more peripheral areas of the macula showed a stronger association with glaucoma than did the more central macula . The study , also showed that the inferior NFL was the parameter most strongly associated with glaucoma status . It is a well known fact that optic nerve defects associated with glaucoma often occur initially at the inferior pole and that VF defects associated with glaucoma frequently manifest first in the superior VF , corresponding to the inferior pole defects .

The limitation of the study is the lack of age matched controls from the normal population .It compares the pre-existing normative database of the machine in the presenting population of the clinic . So a similar study with inclusion of normal population as age matched controls would possibly make the results more specific , classification of glaucoma suspects further into categories like ocular hypertension , glaucoma suspects and early glaucoma in subsequent trials in glaucoma diagnosis would make the use of OCT much more useful and rewarding for the present day ophthalmologists in treating the disease .

The study results support zeimer et al 's hypothesis that macular thickness is reduced in glaucoma .Conversely , we found that peripapillary NFL thickness is a more sensitive indicator of the presence or absence of glaucoma than was macular thickness .Nevertheless , macular thickness assessment clearly may have a role in the assessment and diagnosis of glaucoma .

	No. of Eyes	**Mean age (yrs)**	**Mean IOP (mm hg)**	**Total macular volume (Cubic mm)**	**Avg Retinal thickness (μm)**	**Mean macular thickness (μm)**
POAG suspects	**142**	**46.68± 12.24**	**18.36±4.43**	**6.83±0.58**	**94.55±14.5**	**240.39 ± 14.04**
POAG	**148**	**52.66±12.12**	**18.22±4.74**	**6.35±0.49**	**81.58±20.13**	**224.23 ± 17.55**

Summary of reports in the literature on macular thickness and volume and Retinal NFL thickness in normal and glaucomatous eyes using OCT.

Author	**Scan Protocol**	**No.of.eyes**	**Results**		
Joel S. schuman et al[77]	Prototype OCT	534 (166 – normal, 83- suspects, 196-early, 89-advanced)	**Diagnosis**	Mean macular thickness μm(SD)	Mean RNFL thickness μm(SD)
			Normal	229.0 (13.4)	113.6 (15.8)
			Suspects	224.9 (16.0)	106.0 (18.9)
			Glaucomatous	214.5 (17.0)	64.3 (27.3)

Author	Scan Protocol	No.of.eyes	Diagnosis	Results	
				Mean macular thickness μm(SD)	Mean RNFL thickness μm(SD)
Joel S. schuman et al[68]	Prototype OCT	10 (10-normal)	Normal	235 (9.8)	98 (9)
Harmohina Bagga et al [69]	Prototype OCT	59 (29- normal, 30 – glaucomatous)	Normal	304 (15)	140 (14)
			Glaucomatous	278 (24)	91 (31)
David S. Green field et al [70]	Prototype OCT	40 (20- normal, 20 –glaucomatous)	Normal	243.5 (15)	105.6 (19)
			Glaucomatous	220.4 (11.3)	49.6 (15.9)
Our study	Prototype OCT	290 (142 - POAG suspects 148 – POAG)	Suspects	240.39 (14.04)	94.5 (14.5)
			Glaucomatous	224.23 (17.55)	81.58 (20.1)

Author	Scan Protocol	No.of.eyes	Results		
			Total Macular Volume Cu.mm (SD)		Minimum foveal thickness μ m (SD)
Tewari et al [76]	Prototype OCT	170 (170- normal)	Normal	6.486 (0.56)	149.16 (21.1)
Our study	Prototype OCT	290 (142 - POAG suspects 148 – POAG)	Suspects	6.83 (0.58)	167.52 (36.1)
			Glaucomatous	6.35 (0.49)	160.62 (22.7)

CONCLUSION

Macular retinal thickness as measured by OCT was capable of detecting glaucomatous damage and corresponded with peripapillary NFL thickness .

Glaucoma is a complex multifactorial disorder characterized by a typical pattern of optic nerve damage and visual field loss that is usually but not always associated with elevated IOP . Accepted parameters for monitoring glaucoma include descriptions and photography of the optic disc appearance (cup disc ratio), measurement of IOP , and periodic threshold perimetry . Advances in posterior segment imaging technology provides a means for generating structural data useful in monitoring eyes with glaucomatous optic nerve damage. Objective, quantitative measurements of optic nerve and surrounding RNFL generated with these technologies correlate with known characteristics of optic disc function and visual function .

Based on our findings we do not recommend the routine use of OCT macular scanning alone for glaucoma detection unless there are ocular pathologies that prevent scanning of the peripapillary region . Conversely , because macular retinal thickness corresponds well with peripapillary NFL thickness , macular scanning can provide a confirmation of abnormalities detected by peripapillary OCT scans . Especially in subtle cases , particularly those with minimal or no perimetric findings , macular and peripapillary scans may reinforce each other in conforming the presence of early abnormalities .

The result of this report suggest that macular thickness measurements generated with OCT represent a neglected structural end point for glaucoma. Although glaucoma is a optic

nerve disorder, the fundamental defining abnormality is localized at the level of retinal ganglion cell. Glaucoma is known to cause loss of ganglion cells and their axons ,leading to a reduction in thickness of the RNFL . Macular thickness measurements represent a surrogate indicator of retinal ganglion cell thickness and could prove to have clinical value for glaucoma diagnosis and detection of change . Our results support this hypothesis and illustrate a significant correlation between macular thickness and two established indicators of glaucomatous damage –RNFL loss and loss of VISUAL FIELD .

We have found significant difference in mean macular thickness between POAG SUSPECTS and patients with established POAG using OCT . Furthermore ,macular thickness and RNFL thickness assessments were strongly correlated with visual field global indices .

OCT provides high resolution ,cross sectional imaging of the retina and the RNFL . A high level of correlation between OCT –generated RNFL thickness and visual function has been reported by several authors .It is important to emphasize that macular thickness measurements have limited use monitoring glaucoma in eyes with macular co-morbidity . Thus , eyes with diabetic or age related maculopathy are not candidates for monitoring macular thickness changes as a strategy for glaucoma diagnosis or detection of glaucomatous progression .

OCT is unique because it provides a non contact , transpupillary approach for directly imaging the cross sectional microstructure of the retina through a time of flight measurement , with a resolution of approximately 10 microns . No reference plane is required since OCT provides an absolute measurement of retinal substructure and determination of NFL thickness

and macular thickness directly from image data .

In conclusion, macular thickness changes are well correlated with changes in visual function and RNFL structure in glaucoma and may represent a surrogate indicator of retinal ganglion cell loss. Hence Macular thickness measurements with OCT may provide a new approach for detection and monitoring of glaucoma in case of diagnostic dilemma.

Future goals in this direction include the creation of new algorithm to specifically measure the macular NFL/ ganglion cell layer, or ganglion cell layer alone, and the development of ultra-high resolution OCT devices (2-3 μm) to actually image and count ganglion cells. The recognition of the importance and benefits of macular thickness measurements in glaucoma represents a new approach to the evaluation and management of the disease.

BIBLIOGRAPHY

j) Quigley HA: Number of people with glaucoma worldwide. Br J Ophthalmol 80:389, 1996

k) Thylefors B, Negrel AD: The global impact of glaucoma. Bull world Health Organ 72: 323, 1994

l) American Academy of Ophthalmology: Primary open-angle glaucoma: preferred practice pattern, San Francisco, 1996, The Academy.

m) Schuman SJ et al: Quantification of Nerve Fibre layer thickness in normal and glaucomatous eyes using Optical Coherence Tomography. Arch Ophthalmol 113:586-596, 1995

n) Quigley HA, Addicks EM, Green WR. Optic nerve damage in human glaucoma, III: quantitative correlation of nerve fibre loss and visual field defect in glaucoma, ischemic neuropathy, papilledema, and toxic neuropathy. Arch Opthalmol. 1982; 100:135-146

o) Lichter PR. Variability of expert observers in evaluating the optic disc. Trans Am Ophthalmol Soc. 1976; 74:532

p) Mikelberg FS, Airaksinen PJ, Douglas GR, Schulzer M, Wijsman K., The correlation between optic disk topography measured by the videoophthalmograph (Rodenstock analyzer) and clinical measurement. Am J Ophthalmol. 1985; 100:417

q) Shields MB et al, Reproducibility of topographic measurements with the optic nerve

head analyzer. Am J Ophthalmol. 1987; 104:581

r) Caprioli J et al., Reproducibility of optic disc measurements with computerized analysis of stereoscopic video images. Arch Ophthalmol. 1986; 104:1035-1039

s) Shields MB. The future of computerized image analysis in the management of glaucoma. Am J Ophthalmol. 1989; 108:319

t) Airaksinen PF, Drance SM, Schulzer M., Neuroretinal rim area in early glaucoma. Am J Ophthalmol. 1985; 99:1

u) Caprioli J, et al. Videographic measurements of optic nerve topography in glaucoma. Invest ophthalmol Vis sci. 1988; 29:1294

v) Caprioli J, et al. Measurements of peripapillary nerve fibre layer contour in glaucoma. Am J Ophthalmol. 1989; 108:404

w) Bille JF, Dreher AW, Zinser G., Scanning laser tomography of the living human eye. In Masters BR, ed. Noninvasive Diagnostic Techniques in Ophthalmology. New York, NY: Springer-Verlag NY Inc; 1990; 29:1294

x) Huang D, Swanson EA, Lin CP, et al. Optical coherence tomography. Science 1991; 254:1178-1181

y) Chauhan DS, Marshall J. The interpretation of Optical coherence tomography images of the retina. Invest Ophthalmol Vis Sci 1999; 40:2332-2342

z) Pieroth L, Schuman JS, Hertzmark E, et al. Evaluation of focal defects of the nerve fibre layer using Optical coherence tomography: a pilot study. Arch Ophthalmol. 1995; 113:586-596

aa) Zangwill LM, Williams J, Berry CC, et al., A comparison of Optical coherence tomography and retinal nerve fibre layer photography for detection of nerve fibre layer

damage in glaucoma. Ophthalmology 1999; 106:570-579

bb) Hon ST, Greenfield DS, Mistlberger A, et al. Optical coherence tomography and scanning laser polarimetry in normal, ocular hypertensive, and glaucomatous eyes. Am J Ophthalmol 2000; 129:129-135

cc) Bowd C, Weinreb RN, Williams JM et al., The retinal nerve fibre layer thickness in ocular hypertensive, normal and glaucomatous eyes with Optical coherence tomography. Arch Ophthalmol 2000; 118:22-26

dd) Soliman MAE, Van Den Berg TJTP, Ismaeil LA, et al. Retinal nerve fibre layer analysis: relationship between Optical coherence tomography and red-free photography. Am J Ophthalmol 2002; 133:187-195

ee) Quigley HA, Dunkelberger GR, Green WR. Retinal ganglion cell atrophy correlated with automated perimetry in human eyes with glaucoma. Am J Ophthalmol 1989; 107; 453-464

ff) Helmholtz H. Beschreiburg eines augenspiegels zur untersuchung der netzhaut in lebnden augie. Berlin, A. Forstner, 1851

gg) Lichter PR. Variability of expert observers in evaluating the optic disc. Trans Am Ophthalmol Soc 1976;74:532

hh) Tielsch JM, Schwartz B. Reproducibility of photogrammetric optic disc cup measurements. Invest Ophthalmol Vis Sci 1985;26:814

ii) Varma R, Spaeth GL. The PAR IS 2000. A new system for retinal digital analysis. Ophthalmic Surgery 1988;19:1183

jj) Dandona L, Quigley HA, Jampel HD. Reliability of optic nerve head topographic measurements with computerized image analysis. Am J Ophthalmol 1989;108:414

kk) Bishop KI, Werner EB, Krupin T, et al. Variability and reproducibility of optic disc topographic measurements with the Rodenstock Optic Nerve Head Analyzer. Am J Ophthalml 1988;106:696

ll) Belyea DA, Dan JA, Lieberman MF, et al. The Glaucoma-scope: Reproducibility and accuracy of results. Invest Ophthalmol Vis Sci 1994;35:429

mm) Hamzavis S, Stewart WC, Thompson TL. Inter and intraobserver variation of the optic nerve head in cadaver eyes using the Glaucoma-scope. Invest Ophthalmol Vis Sci 1993;35 (suppl): 427

nn) Takamoto T, Netland PA, Schwartz B. Comparison of measurements of optic disc cup by glaucoma scope and stereophotogrammetry. Invest Ophthalmol Vis Sci 1993;35(suppl): 433

oo) Balazsi GA, Drance SM, Schulzer M, et al. Neuroretinal rim area in suspected glaucoma and early chronic open angle glaucoma. Arch Ophthalmol 1984;102:1011

pp) Caprioli J, Ortiz-Colberg R, Miller JM, Tressler C. Measurements of Peripapillary nerve fibre layer contour in glaucoma. Am J Ophthalmol 1989;108:404

qq) Shields MB, Martone JF, Shelton AR, et al. Reproducibility of topographic measurements with the optic nerve head analyzer. Am J Ophthalmol 1987;104:581

rr) Shields MB, Tiedeman JS, Miller KN, et al. Accuracy of topographic measurements with the optic nerve head analyzer. Am J Ophthalmol 1989;107:273

ss) Plesch A, Klingbeil U, Rappl W, et al. Scanning ophthalmic imaging. In Nasmann JE, Burk ROW (eds). Scanning laser ophthalmoscopy and tomography. Munchen, Quintessenz, 1990, p 23-37

tt) Webb RH, Hughes GW, Delori FC. Confocal scanning laser ophthalmoscope. Applied

Optics, 1987;26:1492

uu) Peli E. Electro-optic fundus imaging. Surv Ophthalmol, 1989;34:113

vv) Kino GS, Corle TR. Confocal scanning optical microscopy. Physics Today 1989;42:55

ww) Masters BR, Kino GS. Confocal microscopy of the eye. In Masters BR (ed). Noninvasive Diagnostic Techniques in Ophthalmology. New York, Springer-Verlag, 1990, pp 152-171

xx) Schuman H, Murray JM, Di Lullo C. Confocal microscopy. An overview. Bio Techniques 1989;7:154

yy) Billie JF, Dreher GW, Zinser G. Scanning laser tomography of the living human eye. In Masters BR (ed); Noninvasive Diagnostic Techniques in Ophthalmology. New York, Springer-Verlag, 1990, pp 528-547

zz) Dreher AW, Tso PC, Weinreib RN. Reproducibility of topographic measurements of the normal and glaucomatous optic nerve head with the laser tomographic scanner. Am J Ophthalmol, 1991;111:221

aaa) Mikelberg F, Wijsman K, Schulzer M. Reproducibility of topographic parameters obtained with the Heidelberg retina tomography. J Glaucoma, 1993;2:101-103

bbb) Quigley HA, Addicks EM, Green WR. Optic nerve damage in human glaucoma. Arch Ophthalmol 1982;100:135

ccc) Quigley HA, Addicks EM. Quantitative studies of retinal nerve fibre layer defects. Arch Ophthalmol 100:807-814,1982

ddd) Quigley HA, Miller NR, George T. Clinical evaluation of nerve fibre layer atrophy as an indicator of glaucomatous optic nerve damage. Arch Ophthalmol,1980;98:1564-1571

eee) Reiter K, Dreher AW, Weinreb RN. Accuracy and reproducibility of a retinal laser

ellipsometer. Invest Ophthalmol Vis Sci 1991;32(suppl):812

fff) Dreher AW, Reiter K, Weinreb RN. Spatially resolved birefringence of the retinal nerve fibre layer assessed with a retinal laser ellipsometer. Applied Optics 1992;31:3730-3735

ggg) Weinreb RN, Dreher AW, Coleman A, et al. Histopathologic validation of Fourier-ellipsometry measurements of retinal nerve fibre layer thickness. Arch Ophthalmol 1990;108:557

hhh) Dreher AW, Reiter K. Retinal laser ellipsometry: A new method for measuring the retinal nerve fibre layer thickness distribution? Clinical Vision Sciences,1992;7: 481-488

iii) Morsman CD, Karwatowski WSS, Wienreb RN. Reproducibility of retinal nerve fibre layer thickness measurements by scanning laser polarimetry and correlation with red free photography in normal eye. Invest Ophthalmol Vis Sci 1993;34(suppl):1507

jjj) Zeimer R, Shahidi M, Mori M, et al. A new method for rapid mapping of the retinal thickness at the posterior pole. Invest Ophthalmol Vis Sci 1996;37:1994-2001

kkk) Schuman JS, Kim Joshua, Imaging of the optic nerve head and nerve fibre layer in glaucoma. Ophthalmol Clinics of North America, 2000;13:383-406.

lll) Werner EB, Interpreting automated visual fields. Ophthalmology Clinics of North America. 1995; 8:229-258

mmm) Heijl A et al. Extended empirical statistical package for evaluation of single and multiple fields in glaucoma: Statpac2. Perimetry update 1991, pp 303-315

nnn) Heijl A: Reliability parameters in computerized perimetry. Seventh International Visual Field Symposium, 1987, pp 593-600

ooo) Heijl A: A package for the statistical analysis of visual fields. Seventh International

Visual Field Symposium, 1987, pp 153-168

ppp)Flammer J. The concept of visual field indices. Graefes Arch Clin Exp Ophthalmol, 1986; 224:389-392

qqq)Heijl A, et al. A package for the statistical analysis of visual fields. Seventh International Visual Field Symposium, 1987, pp 153-168

rrr)Aman P, Heijl A. Glaucoma hemifield automated visual field evaluation. Arch Ophthalmol 1992; 110: 812-819

sss)Asman P, Heijl A. Evaluation of methods for automated hemifield analysis in perimetry. Arch Ophthalmol 1992; 110: 820-826

ttt) Anderson DR. Automated Static Perimetry. St. Louis, MO, Mosby Year Book 1992, pp 10-93

uuu)Radius RL. Anatomy and pathophysiology of the retina and the optic nerve. The Glaucomas. St. Louis, CV Mosby, 1989, pp 89-132.

vvv)Lindenmuth KA, et al. Effects of papillary constriction on automated perimetry in normal eyes. Ophthalmology, 1989; 96:1298-1301

www)Searle AET, Wild JM, Shaw DE, et al. Time-related variation in normal automated perimetry. Ophthalmology 1991; 98: 701-707

xxx)Obuchowski Nancy A., Receiver Operating Characteristic curves and their use in Radiology, 2003; 229: 3-8.

yyy)Joel S. Schuman et al . Reproducibility of NFL thickness , macular thickness and optic nerve head measurements using Stratus OCT .IOVS 2004,1716-1724.

zzz)Harmohina Bagga et al .Macular thickness changes in glaucomatous optic neuropathy detected using OCT .Arch Ophthalmology 2003;121,41-46.

aaaa)David S. Greenfield et al . Quantitative assessment of structural damage in eyes with localized VF abnormalities . AJO 2004,797-805.

bbbb)Ophthalmology 2nd edition ,Myron Yanoff ,Jay S. Duker.

cccc)American Academy Of Ophthalmology, Glaucoma section.

dddd)Glenn J. Jaffe , et al. Optical coherence tomography to detect and manage retinal diseases and glaucoma.AJO 2004;137,156-168.

eeee)Zeimer et al, Quantitative detection of glaucomatous damage at the posterior role by Retinal thickness mapping. A pilot study. Ophthalmology 1998; 105:224-231.

ffff)Zeimer et al. A new method for rapid mapping of the retinal thickness at the posterior pole. IOVS, 1996;37:1994 – 2001.

gggg)Vijay B Wagh, Parul Sony, Hem K. Tewari et al. Macular thickness evaluation using the optical coherence tomography in normal Indian eyes. IJO 2004; 52:199-204.

hhhh)Guedes V, Joel S. Schuman et al. Optical Coherence Tomography measurement of macular and nerve fiber layer thickness in normal and glaucomatous human eyes. Ophthalmology 2003;110:177-189.